REPORT DOCUMENTATION PAGE

Form Approved
OMB No. 0704-0188

PLEASE DO NOT RETURN YOUR FORM TO THE ABOVE ORGANIZATION.

1. REPORT DATE *(DD-MM-YYYY)*	2. REPORT TYPE	3. DATES COVERED *(From - To)*
30-11-2007	Journal Article	

4. TITLE AND SUBTITLE
Measurements of Storm and Non-Storm Circulation in the Northern Adriatic: October 2002 - April 2003

5a. CONTRACT NUMBER

5b. GRANT NUMBER

5c. PROGRAM ELEMENT NUMBER
0602435N

6. AUTHOR(S)
Jeffrey W. Book, Richard P. Signell, Henry Perkins

5d. PROJECT NUMBER

5e. TASK NUMBER

5f. WORK UNIT NUMBER
73-6648-06-5

7. PERFORMING ORGANIZATION NAME(S) AND ADDRESS(ES)
Naval Research Laboratory
Oceanography Division
Stennis Space Center, MS 39529-5004

8. PERFORMING ORGANIZATION REPORT NUMBER
NRL/JA/7330--06-6144

9. SPONSORING/MONITORING AGENCY NAME(S) AND ADDRESS(ES)
Office of Naval Research
800 N. Quincy St.
Arlington, VA 22217-5660

10. SPONSOR/MONITOR'S ACRONYM(S)
ONR

11. SPONSOR/MONITOR'S REPORT NUMBER(S)

12. DISTRIBUTION/AVAILABILITY STATEMENT
Approved for public release, distribution is unlimited.

13. SUPPLEMENTARY NOTES

14. ABSTRACT
Fifteen bottom-mounted Acoustic Doppler Current Profilers were deployed from October 2002 through April 2003 in the northern Adriatic Sea. Average transport from the portion of the Western Adriatic Current (WAC) along the Italian slope was 0.1470 ± 0.0043 Sv, punctuated by bursts of more than twice that amount during storm events. Monthly means were calculated with times f strong wind-driven circulation excluded. These suggest a 2002/2003 seasonal separation consisting of October, December through February, and March through April. An extreme Po River flood influenced November conditions making seasonal categorization difficult. October generally had more kinetic energy and more vertical structure than other months, and near-inertial waves were more frequent in April and October. The Eastern Adriatic Current (EAC)/WAC system was clearly present in the means for all months. The cyclonic gyre north of the Po River was present October through February . Generally, in the WAC, over 50% of kinetic energy came from vertically uniform monthly mean flows. Strengthening of both EAC and WAC also occurs during sirocco storms.

15. SUBJECT TERMS
Adriatic, currents, wind-storms

16. SECURITY CLASSIFICATION OF:			17. LIMITATION OF ABSTRACT	18. NUMBER OF PAGES	19a. NAME OF RESPONSIBLE PERSON
a. REPORT	b. ABSTRACT	c. THIS PAGE			Jeffrey Book
Unclassified	Unclassified	Unclassified	UL	20	19b. TELEPHONE NUMBER *(Include area code)* 228-688-5251

JOURNAL OF GEOPHYSICAL RESEARCH, VOL. 112, C11S92, doi:10.1029/2006JC003556, 2007

Measurements of storm and nonstorm circulation in the northern Adriatic: October 2002 Through April 2003

J. W. Book,[1] Richard P. Signell,[2,3] and Henry Perkins[1,4]

Received 17 February 2006; revised 24 January 2007; accepted 7 June 2007; published 16 November 2007.

[1] Fifteen bottom-mounted Acoustic Doppler Current Profilers were deployed from October 2002 through April 2003 in the northern Adriatic Sea. Average transport from the portion of the Western Adriatic Current (WAC) along the Italian slope was 0.1470 ± 0.0043 Sv, punctuated by bursts of more than twice that amount during storm events. Monthly means were calculated with times of strong wind-driven circulation excluded. These suggest a 2002/2003 seasonal separation consisting of October, December through February, and March through April. An extreme Po River flood influenced November conditions making seasonal categorization difficult. October generally had more kinetic energy and more vertical structure than other months, and near-inertial waves were more frequent in April and October. The Eastern Adriatic Current (EAC)/WAC (i.e. inflow/outflow) system was clearly present in the means for all months. The cyclonic gyre north of the Po River was present October through February. Generally, in the WAC, over 50% of kinetic energy came from vertically uniform monthly mean flows. Elsewhere, eddy kinetic energy was stronger than mean kinetic energy with 10–40% contributions for vertically uniform monthly mean flows, 40–60% for vertically uniform monthly varying flows, and 10–30% for vertically varying monthly varying flows. Mean currents for bora storms indicate enhancement of the EAC/WAC and the cyclonic northern gyre, a shift toward Kvarner Bay in EAC direction, a circulation null point south of the Po, and double-gyre bifurcation of flow at Istria. Strengthening of both the EAC and WAC also occurs during sirocco storms.

Citation: Book, J. W., R. P. Signell, and H. Perkins (2007), Measurements of storm and nonstorm circulation in the northern Adriatic: October 2002 Through April 2003, *J. Geophys. Res., 112*, C11S92, doi:10.1029/2006JC003556.

1. Introduction

[2] The circulation of the northern Adriatic Sea is heavily influenced by repetitive bursts of strong wind forcing, making this area a prototype of a wind-forced, shallow marginal sea. Because of the nearness of coastal boundaries, the general circulation and the ocean response to strong winds in such seas is often inherently linked to basin-scale dynamics and cannot be properly understood outside of this broader context. Thus basin-scale observations are needed to understand the circulation and response, and to evaluate numerical modeling predictions.

[3] The northern Adriatic is characterized by depths of a few tens of meters, increasing gradually toward the mid-Adriatic Pit. The western coastline is mostly featureless except for the Po River delta near 45°N. The northern coastline has several lagoons that have limited connection to the open sea. The semienclosed shallow area in the northeast corner is the Gulf of Trieste. The irregular eastern coastline is marked by the mountainous Istrian Peninsula and numerous islands and bays. Depths in and around these bays are sometimes greater than 80 m. The bay southeast of Istria, Kvarner Bay, is 50 m deep and connects to the rest of the northern Adriatic through a 30 km wide passage. The other bays connect to the northern Adriatic and to each other through passages that are much narrower than the Kvarner Bay passage, but are comparable to it in depth. Figure 1 shows the bathymetry and features of the northern Adriatic.

[4] The general circulation of the Adriatic is cyclonic with southeastward flows along the western side of the sea and northwestward flows along the eastern side [*Orlić et al.*, 1992]. The northern Adriatic includes the northernmost portion of this Eastern Adriatic Current (EAC) and Western Adriatic Current (WAC) system. Near the southern tip of Istria, in all seasons, the EAC turns southwestward to cross the sea, joining outflow water from the Po River and becoming the WAC [*Poulain*, 2001]. In agreement with *Poulain* [2001] the WAC is here defined as the entire southeastward current along the Italian side of the sea. An isolated cyclonic gyre spanning the width of the basin to the northeast of the Po River is the most prominent mean circulation feature not directly part of the EAC/WAC system. *Cushman-Roisin et al.* [2001] present a comprehensive review of the physical oceanography of the northern Adriatic.

[1] Naval Research Laboratory, Stennis Space Center, Mississippi, USA.
[2] NATO Undersea Research Centre, La Spezia, Italy.
[3] Now at U.S. Geological Survey, Woods Hole, Massachusetts, USA.
[4] Now at School of Marine Sciences, University of Maine, Walpole, Maine, USA.

0148-0227/07/2006JC003556$09.00

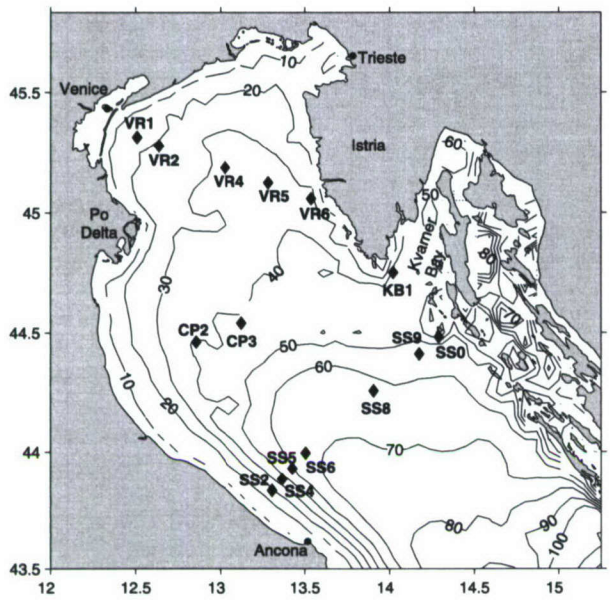

Figure 1. Locations of moorings (black diamonds), northern Adriatic bathymetry, and place names used in the paper. SS10 is labeled as SS0 here and in following figures for ease of display.

[5] Several studies have calculated the seasonal variability of Adriatic circulations using hydrographic observations [e.g., *Artegiani et al.*, 1997b]. However, as noted by *Orlić et al.* [1992], transient wind-driven currents in the Adriatic may surpass the thermohaline circulations by an order of magnitude. Therefore current measurements are needed to properly access the seasonality of the total currents and the contributions to the mean of the strong transient wind-driven currents. *Poulain* [2001] produced maps of seasonal currents and analyzed the mean and eddy kinetic energies of the Adriatic using a decade of surface drifter measurements. However the nature of these drifter measurements limits the scope of this climatology to surface currents. Until recently, technological and political challenges have prevented long-term, basin-scale observations of currents throughout the water column.

[6] Currents in the northern Adriatic are heavily influenced by wind, and the wind that is most prevalent during winter blows southwestward over the sea from the mountains along the east coast. These winds, called bora, affect the northern Adriatic by changing its circulation for short periods during and following events. Bora winds have strong horizontal shear from interactions with the complex mountainous east coast topography. *Zore-Armanda and Gačić* [1987] analyzed current meter records in the northern Adriatic under bora conditions and suggested that this wind shear acts on the ocean to form two gyres. The first gyre is the cyclonic one northeast of the Po River previously discussed. The second is an anticyclonic gyre which forms from the Po River to the southern half of the coast of Istria. The limited domain model of *Kuzmić and Orlić* [1987] and the full Adriatic model of *Orlić et al.* [1994] predicted such a double-gyre system during bora conditions, in agreement with measured currents. Recent modeling studies by *Beg Paklar et al.* [2001] and *Pullen et al.* [2003] used high-resolution wind forcing to reproduce more complex and realistic features of the ocean response to bora.

[7] The other strong wind of the Adriatic is the sirocco, which blows from the southeast along the axis of the sea [see *Guymer and Zecchetto*, 1993, Figure 14]. Sirocco events can cause storm surge flooding in Venice and they have been studied both numerically and theoretically by many scientists. According to *Finizio et al.* [1972] and *Poje and Hrabak-Tumpa* [1982] a sirocco has shear such that maximum wind speeds occur on the Croatian side of the sea. The paper of *Orlić et al.* [1994] predicts upwind flow in the deeper areas of the northern Adriatic and downwind flow in the shallower areas as long as the sirocco wind shear from Italy to Croatia is not too large. This implies a weakening of the WAC circulation near the coast in agreement with limited measurements made by *Artegiani et al.* [1983] and V. Kovačević [*Cushman-Roisin et al.*, 2001, Figures 3–10] and the model of *Betello and Bergamasco* [1992].

[8] This paper analyzes current measurements taken over a 7 month period in terms of monthly statistics. Strong sirocco and bora wind events are also examined in terms of their own statistics and their impact on the means and variability of the circulation. Section 2 describes the measurements used in the study; section 3 presents calculations of WAC transport; section 4 presents monthly means; section 5 discusses the distribution of kinetic energy; section 6 discusses the impact of wind storms, and sections 7 and 8 present discussions and conclusions.

2. Measurements

2.1. Moorings and Instrumentation

[9] Bottom-mounted Acoustic Doppler Current Profilers (ADCPs) were deployed by the U.S. Naval Research Laboratory (NRL) during the Adriatic Circulation Experiment (ACE) together with the NATO Undersea Research Centre (NURC) as a Joint Research Project (JRP) from September 2002 to May 2003. ACE/JRP moorings consisted of 14 trawl-resistant bottom-mounted ADCPs [*Perkins et al.*, 2000] distributed throughout portions of four mooring sections. An additional upward looking ADCP was mounted near the base of the meteorological tower described in *Cavaleri* [2000]. These mooring positions are shown in Figure 1 and given in Table 1 with their mean sea level depths. The full mooring sections were populated by both JRP moorings and moorings from international partners collaborating on the study of the northern Adriatic [*Lee et al.*, 2005b]. Instruments on each mooring measured currents throughout the water column (ADCP), bottom temperature (by ADCP and at some sites by wave/tide gauge), and bottom pressure (by ADCP or wave/tide gauge). Additionally, at some locations, measurements were made of bottom salinity (conductivity sensors), bottom pressure from surface waves (wave/tide gauge), and surface wave parameters (ADCP).

2.2. ADCP Current Processing

[10] To reduce surface wave aliasing, JRP ADCPs were set to measure the currents using bursts of pings every 15 min at 1 Hz sampling frequency. The low number of

Table 1. Mooring Positions and Depths

Mooring	Latitude	Longitude	Depth, m
SS2	43.8351°N	13.3066°E	25
SS4	43.8836°N	13.3667°E	46
SS5	43.9307°N	13.4261°E	57
SS6	43.9956°N	13.5044°E	66
SS8	44.2567°N	13.9053°E	65
SS9	44.4102°N	14.1748°E	59
SS10	44.4812°N	14.2904°E	51
CP2	44.4610°N	12.8551°E	42
CP3	44.5402°N	13.1245°E	42
KB1	44.7507°N	14.0213°E	48
VR1	45.3139°N	12.5081°E	17
VR2	45.2789°N	12.6370°E	25
VR4	45.1878°N	13.0281°E	33
VR5	45.1249°N	13.2837°E	35
VR6	45.0581°N	13.5360°E	33

pings per burst that could be sustained for the 7-month deployment duration limited the reduction of measurement noise that could be achieved by averaging pings. A procedure was developed [*Book et al.*, 2007] to remove bad samples from the 15 min ensembles and filter and decimate the data to produce hourly data with reduced noise. Quality control steps to exclude data consisted of internal ADCP tests for exclusion of data with poor signal correlation or fish echo signatures, an objectively determined velocity error cutoff (velocity errors estimated from independent measures of vertical velocity), exclusion of ensembles with more than 40% (20% for surface measurements) of the data marked bad by internal checks, exclusion of rare ensembles with spikes in compass direction, and additional correlation and fish echo tests. The surface echo interference zone was truncated by constructing time series of sea surface height from pressure sensors and acoustic backscatter intensity measurements and using these to exclude measurements at or above the depth of the surface side lobe echo for each measurement time. Linear compass drifts in some records were verified to be false trends by tidal analysis and corrected by small gradual rotations of current vectors (less than 4° at all sites). Data gaps were then removed using a least squares technique that averages neighboring values in depth and time, tides were removed using the response method, and the data were filtered with a 2-hour low-pass, second-order Butterworth filter run forward and backward. Finally, data gaps of more than an hour were reinserted, and the data were decimated to hourly values. *Book et al.* [2007] provides complete details of these processing steps.

[11] At site VR5, extracted tidal ellipses were strongly tilted with respect to tidal ellipses at neighboring stations and the tidal solutions from Navy Coastal Ocean Model (NCOM) simulations run with the Oregon State University tidal database as forcing [*Martin et al.*, 2006]. The tilt of VR5 ellipses also did not agree with predictions by *Janeković and Kuzmić* [2005] from a tidal simulation using the finite element model "Truxton/Fundy" with boundary conditions determined through data assimilation of coastal tide stations. Therefore following the technique described by *Griffin and Thompson* [1996], a strong constraint variational data assimilation scheme was applied to the vertically averaged tides derived from the JRP moorings. This technique tries to adjust model boundary conditions in such a way to match the measured tidal ellipses at VR5 constrained by the dynamics and measurements at other sites. However, as in the other modeling studies, the VR5 ellipses could not be matched. Despite the lack of any physical evidence of instrument malfunction, the tilt disagreement with three independent modeling predictions and with neighboring stations strongly suggests a compass error is present in the VR5 data. Therefore the currents at site VR5 were rotated 28° clockwise to align with the strong constraint variational data assimilation prediction determined from assimilating all JRP tidal mooring data (with the exception of VR5 currents).

3. WAC Transport

[12] It is well known that strong wind events in the northern Adriatic can drastically affect the circulation. Figure 2 illustrates this point; persistent mean currents over particular days with strong wind forcing are many times stronger than the mean flow over the Adriatic season (as defined according to *Artegiani et al.* [1997a]) during which they occur. It is desirable to separate these strong wind periods from more general conditions so that statistics can be calculated separately for different cases and to extend the applicability of the statistics to periods other than October 2002 through April 2003.

[13] *Book et al.* [2005] showed that strong bora storm winds consistently enhance WAC flow along the Italian slope north of Ancona, Italy. Therefore as well as providing interesting results itself, the transport from the portion of the WAC calculated with four JRP moorings closely spaced across this slope is used to detect strong wind storms. COAMPS™ modeled winds [*Martin et al.*, 2006] are used to verify qualitatively that transport peaks were associated with Adriatic wind storms rather than other forcing events. Our purpose in identifying storms in this paper is to develop different cases for ocean statistics rather than for wind statistics. For this purpose an ocean-based technique has an advantage over classification based only on measured or modeled winds because it will include any ocean spin-up and spin-down from short-lived (in terms of wind) storms.

3.1. Transport Methods

3.1.1. Transport Estimation

[14] For the subsection of the WAC considered, the transport over the majority of the water column was calculated from the four moorings (SS2 and SS4–6) by using the assumption that the spatial variability of flow between mooring sites was linear. Thus blocks could be formed between the point of mooring measurement and the midpoint between moorings with the component of velocity perpendicular to the section assigned to the box. Summing the product of the currents and the box areas gives the portion of transport that was directly measured. Near-bottom boxes were truncated horizontally where necessary to prevent them from penetrating the bottom. This truncation was done at the point (within 1 km) where the bottom sloped upward to within an instrument blanking distance from the midpoint (in depth) of the box.

[15] This technique takes advantage of the bin-averaging character of ADCP measurements but leaves out transports

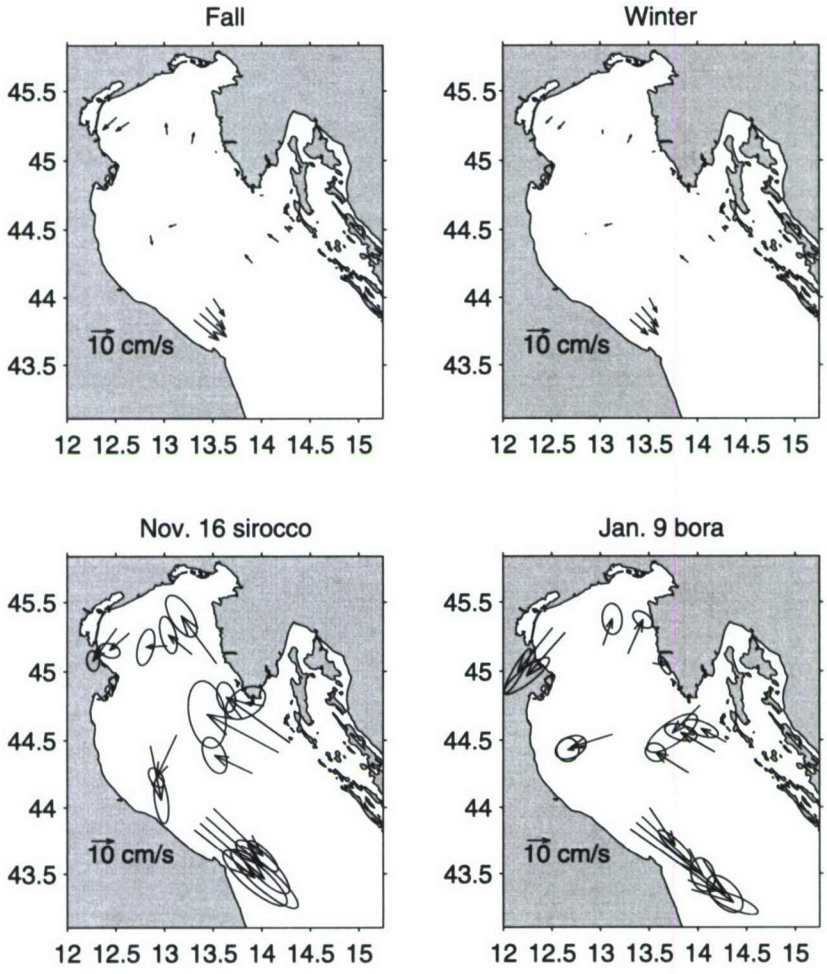

Figure 2. Mean currents observed for fall, winter, a day with strong sirocco wind, and a day with strong bora wind. A velocity-scale vector is drawn in the bottom left of each panel. The ellipses drawn on the sirocco and bora panels are the two-standard-deviation ellipses centered at the mean flow values.

from water above the ADCP surface interference zone, water below the ADCP blanking distance, and water in pockets where the bottom deepens from the measurement point to the midpoint. The transports in the top surface interference zone (5 m or less) were estimated by assuming that the currents in this zone were identical to those measured in the highest-ADCP bin, i.e., an assumption of no shear in the top few meters.

[16] To estimate the transport from the sloping bottom pockets, the velocities from the bounding measurement sites were extrapolated onto a 0.5 m by 1 km grid using the least squares neighbor averaging technique. Then transports were calculated from bins that have a majority of their area not covered by the main blocks or the bottom blanking zone. Finally, to estimate the transports from the bottom blanking zone (typically about 3 m) an estimated "free-stream" velocity was taken at 1 km increments as the velocity from the measured or interpolated box above that portion of the blanking zone. A vertical eddy viscosity coefficient was estimated as 9×10^{-4} m^2/s by fitting time-dependent Ekman layers to measured tidal ellipses near the bottom. Then the transport was estimated for the bottom blanking zone using simple Ekman theory with these values. The median percentage contribution from the combined top and bottom zones to the total transport is 13%. A final 0.1% correction was applied to the total transport to account for the difference in the cross-section area and the combined area of the boxes.

3.1.2. Transport Error Estimation

[17] The error in the transport from the measured portion of the water column can be divided between an error caused by imperfect measurements and an error due to the assumption of linearity between ADCP stations. The first error can be calculated from propagating the random and bias measurement errors and interpolation errors (together on average ±1.5 cm/s) through the transport calculation. The use of four beams by the RDI ADCPs allows this instrument to measure the variance of random error for each bin and the correlation of the random error from bin to bin. The measured correlations for these particular sites are only slightly larger than the expected 15% correlation between adjacent depth bins caused by acoustic bin overlap, and depth correlation length scales are all 1.5 m or less. This suggests that these random errors are dominated by small-

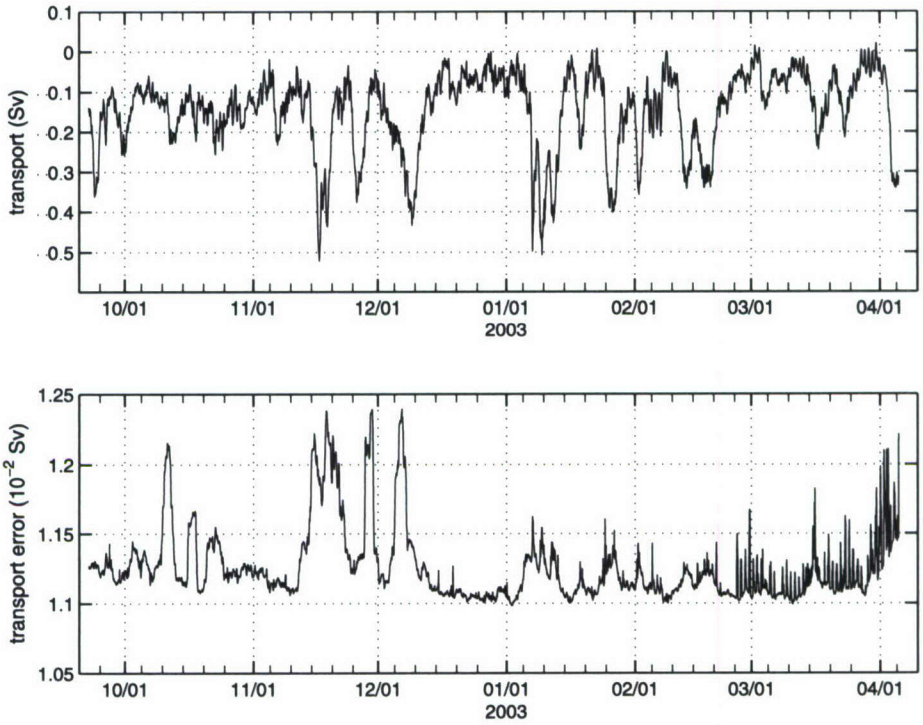

Figure 3. WAC transport (top) and estimated error (bottom panel) over the Italian slope across the section extending from mooring SS2 to SS6. Minor tick marks denote the 5th, 10th, 15th, 20th, and 25th of each month.

scale turbulence effects [e.g., *Lu and Lueck*, 1999]. Bias errors (±0.5% of the currents plus ±0.5 cm/s for 300 kHz ADCPs) are assumed independent between ADCP sites because each ADCP has a different bias. Interpolation errors from data gaps of more than an hour were assigned to the value of the standard deviation of the perpendicular component of velocity at that level. Finally, a ±0.4 cm/s error with a 10 m depth correlation length scale was included to account for measuring currents during bursts rather than continuously. Details of the measurement errors used in these calculations are discussed in *Book et al.* [2007].

[18] The linearity assumption error was estimated from the NCOM simulation described by *Martin et al.* [2006] with tidal fluctuations removed. Transports for the subsection of the WAC were calculated using every 1 km grid point and also using the model values at the moorings sites with linear interpolation. The difference time series between these two transport calculations had a mean of 0.0027 Sv (less outflow using the linear interpolation method), a standard deviation of 0.0099 Sv, and a correlation timescale of 0.9 days. Measurements taken at twice the mooring resolution by a tethered, downward looking ADCP on 28 September 2002 (linear assumption 0.0002 Sv too low) and on 2 October 2002 (linear assumption 0.0036 Sv too low) suggest that the linearity errors estimated from NCOM might be too high. However, the NCOM derived bias and standard deviation are not as limited in spatial resolution or to only two snapshots and are therefore used in the transport error estimate.

[19] The transport error in the top and bottom zones was estimated by comparing different methods for estimating these transports. The alternative methods used to derive the errors were using a linear fit in the top 5 m of measured currents to extrapolate to current values in the top zone, using a Laplace equation extrapolation technique to fill in the 0.5 m by 1 km grid for the bottom pocket boxes, and estimating a "free-stream" velocity by projecting the velocity at the top of the blanking zone upward in the water column using Ekman theory. The standard deviation over 2-day intervals of the differences in transport between these methods and those discussed in section 3.1.1 were combined with the estimates of error derived from the measurements and the linear assumption to produce a total transport error estimation.

3.2. Transport Time Series

[20] Figure 3 shows the results of the transport calculations. Negative transport indicates volume flow toward the southeast, i.e., outflow from the northern Adriatic. The mean transport between moorings SS2 and SS6 was -0.1470 ± 0.0043 Sv for the period of mooring deployment. The transport correlation timescale for the SS2–6 section is 1.9 days and this result was used to estimate both the uncertainty in the mean transport calculation and the standard error of the mean. If the transport variation is statistically stationary, then the expected error in using -0.1470 Sv as the mean for other periods is 0.0144 Sv. On the basis of some preliminary transport estimates (not shown) that make use of JRP data and inshore and offshore rotary current meter data gathered by CNR-ISMAR-Ancona it is estimated that the flow along the slope region spanned

Table 2. Index of Strong Ocean Response to Storms From 22 September 2002 to 5 May 2003

Start Date	Start Time, UTC	End Date	End Time, UTC	Type	Peaks	Maximum Transport, Sv	Maximum Current, cm/s
22 Sep	2100	25 Sep	0200	bora	1	−0.3613	56
14 Nov	2000	20 Nov	0100	sirocco	2	−0.5221	51
24 Nov	2200	28 Nov	0800	sirocco	1	−0.3755	38
03 Dec	1200	12 Dec	0800	bora	1	−0.4337	45
06 Jan	2300	14 Jan	1300	bora	3	−0.5068	80
24 Jan	1800	28 Jan	1500	bora	1	−0.4011	41
01 Feb	0100	03 Feb	0500	bora	1	−0.3568	38
11 Feb	1400	21 Feb	0300	bora	2	−0.3421	40
03 Apr	0100	06 Apr[a]	1800	bora	1	−0.3398	55

[a]Estimated using regression techniques with SS2 and SS5–6 transports only.

by SS2–SS6 is typically about two thirds of the total outflow from the northern Adriatic.

[21] Transport percentage errors are 12% or below for all negative transports with magnitudes greater than 0.1 Sv (i.e. outflow). The median transport percentage error is 9%. The peaks in transport error during the first portion of the record are mainly produced by estimated errors in the surface interference zone transport. These periods of peak error are caused by disagreement between the assumptions of uniform velocity and linear shear for the surface zone during near-inertial oscillation events. After 10 December, near-inertial oscillations with this characteristic are weak or not present and this source of error is reduced. The sharp spikes in error during the latter half of the record occur because the ADCP batteries began to weaken, producing weakened signal strength and higher occurrences of data gaps with durations greater than 1 hour. The linearity assumption error is estimated to have a standard deviation of nearly 0.01 Sv, but this significant random error is represented as constant in Figure 3 (bottom), since its true time variation is unknown.

[22] The transport of the WAC over the Italian slope decreases from September to April with a best fit linear slope of 2.7×10^{-4} Sv per day. However the main source of low-frequency variability is concentrated into several transport events with peaks in WAC slope outflow lasting several days. During these events, WAC slope outflow is 2 or 3 times greater than average. COAMPS reanalysis modeled winds [*Martin et al.*, 2006] were used to verify that each of these events were associated with Adriatic wind storms.

3.3. Strong Ocean Response Storm Index for 2002/2003

[23] To build an index of times of strong ocean response to wind forcing, the WAC slope transport was used to determine periods of northern Adriatic circulation that drastically differed from "normal" conditions. First, periods of outflow transport higher than 0.3 Sv were identified. Then, to include spin-up and spin-down time, the peaks were traced forward and backward to the point at which transport fell below the best fit linear trend line. Each of these events was classified as bora or sirocco storms on the basis of the wind patterns from COAMPS reanalysis [*Martin et al.*, 2006] and the results are shown in Table 2.

[24] For most of the events the durations are too long to match the general meteorological definition of bora [*Dorman et al.*, 2006]. Clearly, the ocean response spins down slower than the wind forcing and bora and sirocco ocean conditions persist for some time after the wind has slowed. In fact, three of the ocean events have multiple, strong peaks in outflow. Each peak is associated with separate wind bursts that are from different bora and sirocco atmospheric events. However these separate bora and sirocco events are spaced so closely in time that the ocean does not fully spin down between events. *Book et al.* [2005] found peak correlation between COAMPS winds off Istria and 16-hour-lagged WAC currents suggesting spin down times of 16 hours or longer. Thus for the ocean, the events are not truly separable and merge to form an extended bora or sirocco period.

[25] The maximum current column in Table 2 was calculated by finding the maximum nontidal vertically averaged current speed at any JRP mooring during the storm event. Although all 15 mooring sites were considered, the maximum always occurred at site SS2 or SS4. Thus the maximum ocean response occurred far away from the peak winds (likely near site KB1) for bora and opposed to the wind direction for sirocco. The strongest bora currents were observed on 7 January, and the strongest sirocco currents were observed on 16/17 November. Peak bora-driven, WAC slope transport occurred on 9 January and peak sirocco-driven, WAC slope transport occurred on 16 November.

4. Monthly Means

4.1. Vertically Averaged Currents

[26] By excluding the storm index periods (section 3.3) from mean calculations, the results should be more representative of typical conditions. As an example, Figure 4 shows the vertically averaged mean currents for November with and without the storms. The general pattern of WAC and EAC flows are the same for both calculations, however the mean strength of the WAC is much reduced for the statistics that exclude the two sirocco storm periods. The sirocco events also alter the pattern of the mean for some sites such as KB1 and VR5. The suggestion of a cyclonic cell northwest of CP2–3 is entirely hidden by the strengthening of the EAC/WAC system by the sirocco (see section 6.1). This revealed cyclonic cell does not appear in other monthly means and is likely caused by the strong Po River outflow event that occurred in November/December. The flood peaked on 30 November with extended periods of strong outflow in November prior to the peak and in December after the peak. However, excluding storm periods, only 38% of the days for November and 9% for December had Po River outflow greater than 4000 m^3/s.

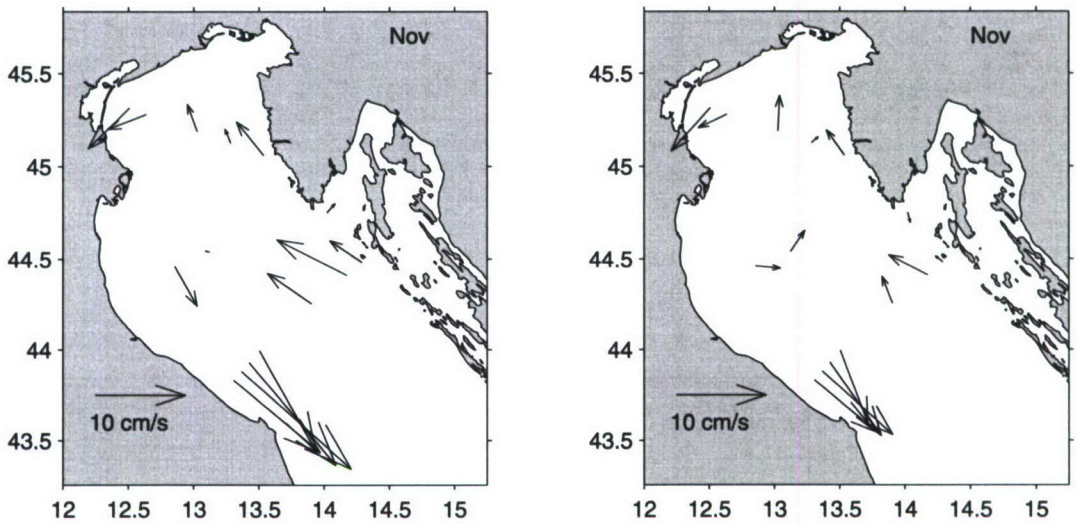

Figure 4. Mean vertically averaged currents for the month of November 2002 including strong storm periods (left) and excluding strong storm periods (right).

Storm periods also significantly alter the mean currents for other months, with the largest change occurring for January.

[27] Figures 5–7 show the vertically averaged mean currents for other months. The EAC/WAC system is clearly present in the means for the SS moorings in all seasons. The cyclonic gyre north of the Po River is also clear in the means for the VR moorings for October through February. However, for March and April this circulation pattern is not present and the mean currents are weak. During October and December the CP mooring means indicate the presence of flow that bounds the north edge of the EAC/WAC gyre. Cross-basin flow is also present at mooring CP3 for February through April, but flow means at CP2 are near zero. The nonstorm means for mooring KB1 indicate outflow from the north side of Kvarner Bay from October through February and inflow from March to April. Tables 3 and 4 present the monthly averaged speed and direction values for these vertically averaged currents. The uncertainties in these quantities are dictated by potential ADCP bias with median uncertainty values of ±0.5 cm/s and ±10° for 300 kHz ADCP sites and ±0.3 cm/s and ±4° for SS2, VR1, and VR4 with higher-frequency ADCPs. Individual speed uncertainties all vary less than 0.1 cm/s from these medians, but individual directional uncertainties vary more because they are inversely proportional to mean speeds (e.g., directional uncertainty for SS5 in November is ±3° and for VR6 in February is ±30°). VR5 directions have higher uncertainties because the velocities were rotated 28° clockwise to

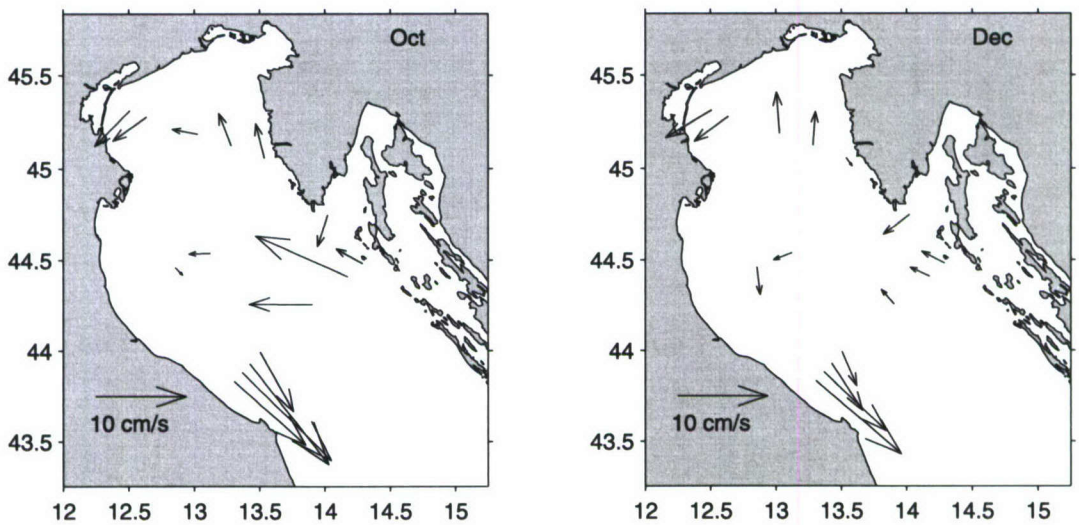

Figure 5. Mean vertically averaged currents excluding strong storm periods for the months of October 2002 (left) and December 2002 (right).

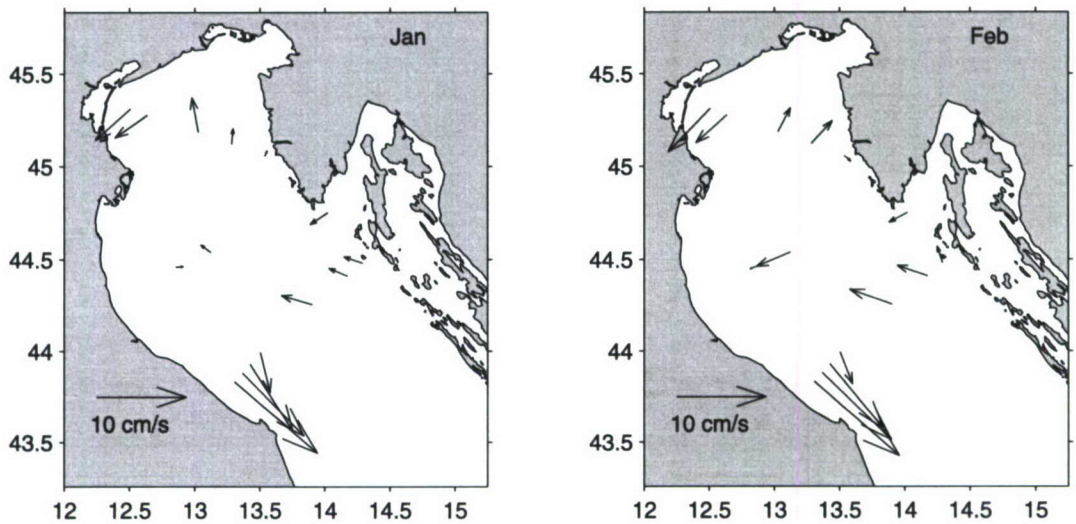

Figure 6. Mean vertically averaged currents excluding strong storm periods for the months of January 2003 (left) and February 2003 (right).

remove suspected bias (see section 2.2). On the basis of tidal ellipse disagreements at other stations, the uncertainty in this rotation is estimated to be ±6°.

[28] Mean currents are not often a good predictor of the speed and direction of the currents at a particular moment for the northern Adriatic. As shown by Figure 8, the variability about the mean in speed and direction is high for all sites even when storm periods are excluded. If the currents were distributed binormally then only 39% of the vectors would fall inside the ellipses of Figure 8. In reality, 48% of the currents fall inside the ellipses indicating a departure from binormal statistics for northern Adriatic currents.

4.2. Vertical Structure of Currents

[29] Figure 9 shows the magnitude of the difference vector between the monthly mean current at a particular depth and the vertically averaged monthly mean current. For a given month, at a particular depth, a nonzero value for this parameter represents a deviation in either current speed or current direction from the vertical mean vector. This parameter represents a velocity form of the energy departures from vertically uniform currents.

[30] The mean currents in October (and to a lesser extent in November) at the WAC sites (SS2–6) had significant shear from the surface to the bottom. Surface flows had higher speeds by 5 cm/s or more than the vertical average

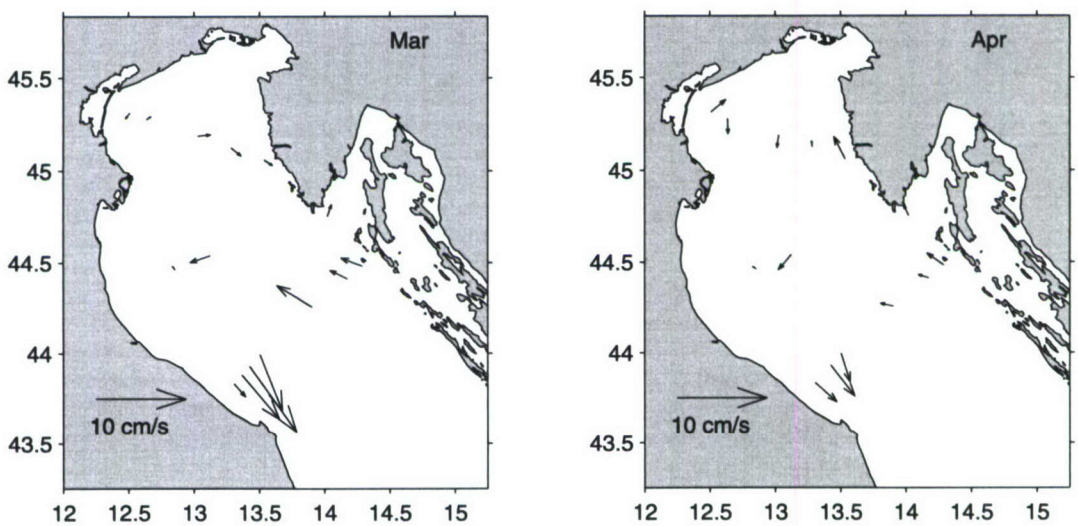

Figure 7. Mean vertically averaged currents excluding strong storm periods for the months of March 2003 (left) and April 2003 (right). April values for site SS4 are not displayed here and in following figures as the ADCP failed in early.

Table 3. Means of Vertically Averaged Currents Given as Speed/Direction[a]

	SS2	SS4	SS5	SS6	SS8	SS9	SS10
Oct	10.7/132	14.0/135	14.2/142	7.6/151	7.1/270	11.2/294	3.4/299
Nov	9.1/130	10.6/132	10.0/145	8.7/159	3.2/338	4.9/297	1.1/308
Dec	12.5/131	9.6/134	6.3/147	4.1/157	2.2/319	2.4/294	2.9/297
Jan	12.2/131	9.8/136	8.8/147	4.6/166	3.6/286	2.3/293	2.2/288
Feb	12.6/131	10.8/134	9.4/140	3.8/159	5.0/289	3.6/289	1.9/341
Mar	1.9/139	6.5/140	9.0/145	6.8/158	4.6/301	2.2/296	2.5/291
Apr	3.2/132	--	4.4/142	3.3/163	1.5/282	1.2/287	2.3/305
Sirocco	21.0/130	30.6/131	27.3/135	22.9/143	14.8/287	18.2/297	12.3/303
Bora	25.9/129	29.8/132	25.5/136	15.2/141	10.0/336	9.5/338	5.3/8

[a]Units for speed are cm/s. Direction is degrees true.

speed and bottom flows had lower speeds by approximately 5 cm/s. This trend is especially accented for the inshore site (SS2) where surface speeds were more than 12 cm/s higher (black indicates off-scale speed in Figure 9). This same form of top to bottom shear in October was also present to a lesser extent at sites SS8–9, KB1, CP2, and VR1. These October and November shears are likely caused by stratification as strong storms have been excluded from these monthly means and the highest shears were measured at sites far from where direct wind forcing was strongest. That is, it is unlikely that these monthly averaged shears can be sustained by any other mechanism except stratification.

[31] CTD (Conductivity-Temperature-Depth) data taken within 5 km of JRP moorings were used to examine these stratification inferences from vertical current shears. The CTD data were collected and shared by various institutions as part of a joint focus on the northern Adriatic during 2002–2003 [*Lee et al.*, 2005b]. Each profile is a snapshot of the stratification at a given time and therefore may or may not represent typical stratification over a month for non-storm times. For October the CTD data generally support the stratification inferences from the currents, as profiles from SS2-5 showed the highest degree of stratification, profiles from SS6-10, CP2, VR1, and VR4, showed moderate stratification, and profiles from CP3, KB1, VR2, and VR5-6 showed weaker stratification.

[32] At site SS5, the speed difference peaks near the bottom for monthly means from December through March. This peak is not caused by a reduction in speed but rather by a speed increase. *Book et al.* [2005] also observed such a peak from an ADCP mooring in nearly this exact location during the winter of 2001. Under geostrophy this implies higher-density waters inshore of SS5 during winter. The observations of a local velocity maximum near 50 m depth around 30 km offshore of Italy both in 2001 and 2003 suggests that this may be a general feature of the WAC system in winter. The peak in speed at depth was also observed to a lesser extent at site SS4 in December, February, and March and at site SS6 in December and March.

[33] Sites SS2, CP2, and VR1 all had significant surface intensification of currents in December, January, and February. These stations are closest to Italy where the Po River plume is generally located. Stratification from this plume appears to have moved offshore to these sites most frequently in winter. At other times it is possible that either the Po plume is not affecting these sites or these sites are completely in the plume from surface to bottom. It is unclear if this result could be extrapolated to other years or if it is only due to the large Po flood that occurred in November/December 2002. A similar peak in speed difference at the surface occurred at site KB1 for these 3 months. This suggests the presence of a front and/or fresh coastal water near the north side of Kvarner Bay during winter. However, frictional wind shear from repeated weak storm events cannot be excluded as a possible explanation for this result because of the mooring's position underneath the expected pathway of the bora wind jet.

[34] Very few CTDs were taken near the JRP moorings from January through March. The limited number of profiles during this period at SS4-10, KB1, and VR5-6 show that the water column was unstratified at these sites during the measurements. Profiles at SS2 for January indicate some stratification in support of the current shear results, but the

Table 4. Means of Vertically Averaged Currents Given as Speed/Direction[a]

	CP2	CP3	KB1	VR1	VR2	VR4	VR5	VR6
Oct	1.2/134	2.4/268	3.8/197	5.5/225	4.6/235	2.9/281	3.9/339	3.9/346
Nov	2.8/95	2.8/34	1.2/166	6.4/222	3.5/245	4.0/3	1.0/49	3.4/325
Dec	3.1/173	2.3/249	3.7/232	6.0/239	4.7/234	4.6/356	3.7/4	1.1/144
Jan	0.8/86	1.4/306	2.3/237	5.2/228	4.4/235	3.9/349	1.7/5	0.7/25
Feb	0.7/248	4.1/247	2.3/242	6.7/224	4.7/229	3.0/27	3.4/43	1.0/132
Mar	0.5/326	2.4/252	1.4/18	0.8/216	0.6/55	1.4/84	1.4/130	1.1/122
Apr	0.5/305	2.3/221	1.3/335	2.2/50	1.7/179	1.4/188	0.6/356	2.8/333
Sirocco	14.7/173	7.7/226	6.6/22	6.4/233	7.2/254	4.3/279	5.5/313	8.2/317
Bora	1.4/245	10.1/256	3.8/285	14.4/224	16.0/224	6.8/347	15.7/19	5.6/112

[a]Units for speed are cm/s. Direction is degrees true.

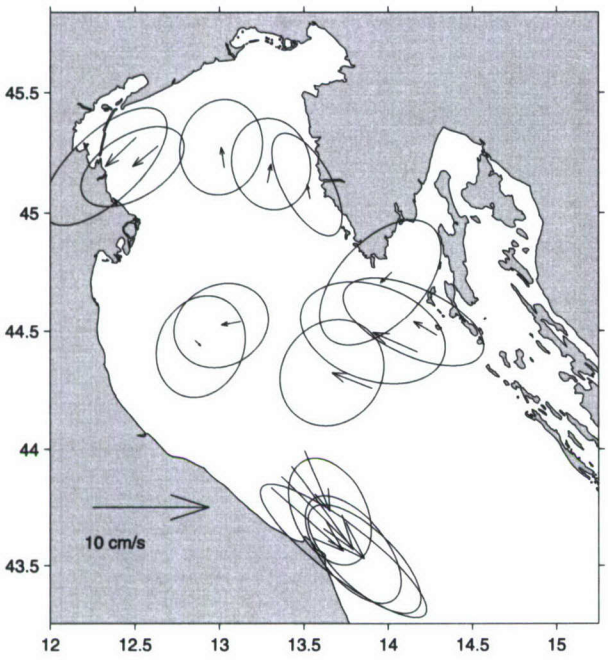

Figure 8. Mean vertically averaged currents excluding strong storm periods for the period from October 2002 through April 2003. One σ standard deviation ellipses are drawn centered at the tip of the mean current vectors.

profiles from February are unstratified. *Lee et al.* [2005a] present TriSoarus towed profile results from cruises of R/V Knorr, including a cruise in February 2003. Profiles near site CP2 show stratification caused by Po plume water overtopping cold dense water. Also, a series of profiles in a radiator pattern were taken just offshore of Kvarner Bay and mooring KB1 during the 11–21 February bora period. The measurements show a complex horizontal frontal system of unstratified water masses. As the winds relax at the end of their survey, the vertical front begins to slump indicating one possible mechanism for the establishment of stratification at site KB1.

[35] With the exception of site SS2, the magnitude of the velocity departures from the vertically averaged velocities was relatively small (usually less than 5 cm/s everywhere) even for the sites discussed above. At other sites and for other months, the magnitudes are often near zero. The monthly mean currents at sites CP3, SS10, VR2, and VR5 remain close to vertically uniform for all months. Current shear was generally very small from December through April for most stations. In March the shear was near zero at all sites, including site SS2.

5. Kinetic Energy Per Unit Mass

[36] Figure 10 shows vertically averaged rotary spectra for the JRP mooring sites. They were calculated from the data before detiding and filtering using the method of *Mooers* [1973] with Welch's averaged periodogram method over block lengths of 512 hours (~21 days) and 50% overlapping Hanning windows. This figure shows significant energies at timescales shorter than 1 month, especially in the inertial oscillation energy band (as indicated by the clockwise rotary peaks at most stations). A mean and eddy kinetic energy division of vertical averages and vertical departures was used to analyze the nontidal variability shown in these spectra and the variance ellipses of Figure 8 with regard to depth dependence and seasonality. At each mooring the currents were divided into four components:

$$\vec{u}(z,t) = \vec{u}^{\ddagger}(t) + \vec{u}^{*}(z,t),$$
$$\vec{u}(z,t) = \overline{\vec{u}^{\ddagger}} + \vec{u}^{\ddagger\prime}(t) + \overline{\vec{u}^{*}}(z) + \vec{u}^{*\prime}(z,t). \quad (1)$$

In this expression, $\ddagger$ is vertical average, * is vertical departure from the vertical average, $\overline{\ }$ is time average over a 1 month period, and $'$ is departure from the monthly time average. Although, $\overline{\vec{u}^{\ddagger}}$ and $\overline{\vec{u}^{*}}(z)$ are not time-dependent within a month, their values do vary from month to month in this method. From these four components, two mean kinetic energy terms and two eddy kinetic energy terms can be derived:

$$\mathrm{MKE}^{\ddagger} = (1/2)\cdot\overline{\vec{u}^{\ddagger}}\cdot\overline{\vec{u}^{\ddagger}},$$
$$\mathrm{EKE}^{\ddagger}(t) = (1/2)\cdot\vec{u}^{\ddagger\prime}(t)\cdot\vec{u}^{\ddagger\prime}(t),$$
$$\mathrm{MKE}^{*}(z) = (1/2)\cdot\overline{\vec{u}^{*}}(z)\cdot\overline{\vec{u}^{*}}(z),$$
$$\mathrm{EKE}^{*}(z,t) = (1/2)\cdot\vec{u}^{*\prime}(z,t)\cdot\vec{u}^{*\prime}(z,t). \quad (2)$$

The "eddies" that contribute to the two eddy kinetic energy terms are defined here to include not only mesoscale eddies but all phenomena where current flow departs from monthly averages.

[37] The vertical average of the monthly averaged total kinetic energy per unit mass can be expressed in terms of these four energy terms:

$$\overline{\mathrm{TKE}^{\ddagger}} = \mathrm{MKE}^{\ddagger} + \frac{1}{T}\sum_{t=1}^{T}\mathrm{EKE}^{\ddagger}(t) + \frac{1}{N}\sum_{z=1}^{N}\mathrm{MKE}^{*}(z) + \frac{1}{TN}\sum_{t=1}^{T}\sum_{z=1}^{N}\mathrm{EKE}^{*}(z,t). \quad (3)$$

5.1. Energy of Vertically Averaged Currents

[38] Figure 11 shows the variation by month and by station for the first two terms of equation (3). All time means in these energy calculations have been calculated excluding the strong storm periods (section 3.3).

[39] Figure 11 (top) is equivalent to an energy representation of the mean currents displayed in Figures 4–7. October (×) had more mean energy in the EAC/WAC system than other months. In general, the vertically averaged mean kinetic energy in the EAC/WAC system was higher than in other locations for all months. In October (×) and November (⋆), WAC flow peaked at sites SS4–SS5; from December through February (◇, *, and ○) WAC flow showed a strong decrease from site SS2 toward offshore; in March (△) and April (□) a weaker WAC flow again peaked offshore of SS2. With the exception of in October, the EAC did not have as distinct spatial peaks in flow as the WAC. Vertically averaged mean kinetic energies were relatively low for all sites outside of the EAC/WAC system. At site

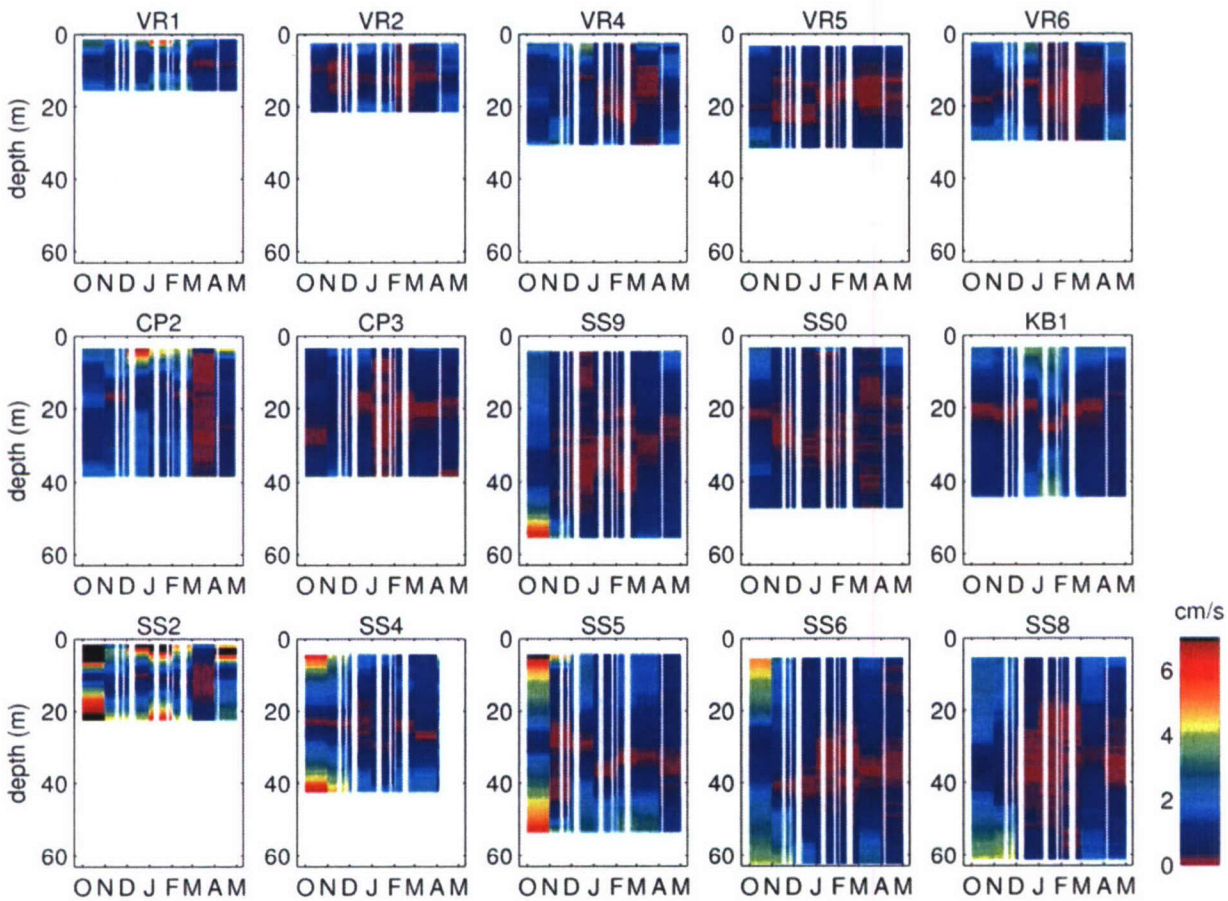

Figure 9. Colors show magnitudes of the monthly mean of vector current difference between observed flow at depth and vertically averaged flow. The x axis tick marks denote the start of each month from October to May. The periods of strong storms that were excluded from the means are indicated as white bars through the monthly blocks. Black indicates off-scale speeds.

VR1, near Venice, the energy did have a modest peak for all months except March and April.

[40] Figure 11 (bottom) shows contributions to the energy budget from vertically uniform "eddy" (i.e., temporally varying) structures with timescales less than 1 month. Barotropic meanders, barotropic eddies, and seiches are examples of events that would contribute to this term. October had the highest energy of this type for most sites. November had high vertically averaged eddy energy at the EAC sites. For the WAC, eddy energy was highest at the inshore site (SS2) with exceptionally high values for January and February. Site KB1 had relatively high eddy energy for all months except April. On the VR section, eddy energy had a local peak at site VR1.

[41] The ratio (not shown) of $\mathrm{EKE}^{\downarrow}(t)$ to MKE‡ is above 3 for all months at sites SS10, KB1, and CP2. Also the ratio is near 2 or higher for all months at sites CP3, VR5 and VR6. In contrast, the ratio is below 2 for all months at the WAC sites of SS4, SS5, and SS6. The median for all sites of this eddy-to-mean kinetic energy ratio rounds to 2 for all months except for March and April. In March the median ratio is 9 and in April it is 6.

5.2. Energy From Vertical Structure of Currents

[42] Figure 12 shows the contributions from the vertical structure terms (last two) of equation (3). Figure 12 (top) shows the additional energy from the nonuniform structure of the monthly mean currents. With the exception of site SS2 in October, these energies are all relatively low. As discussed in section 4.2 the monthly mean currents are relatively uniform with depth through much of the water column for all months.

[43] In contrast, the energy contributions from time-varying vertically structured "eddies" (Figure 12, bottom) are comparable to the energy contributions from time-varying vertically uniform "eddies" (Figure 11, bottom). Examples of events that contribute to the last term in equation (3) include Po plume filaments and eddies, and near-inertial oscillations. The energy in this term for most sites was significantly higher in October than other months, although the energy was also high in April at several sites. In February and March the energy from vertically structured eddies was relatively low at most sites. However, the energy did peak to moderate values near the Italian coast south of the Po (sites CP2 and SS2) in February and near the Italian north coast (sites VR1, VR2, and VR4) in March. The

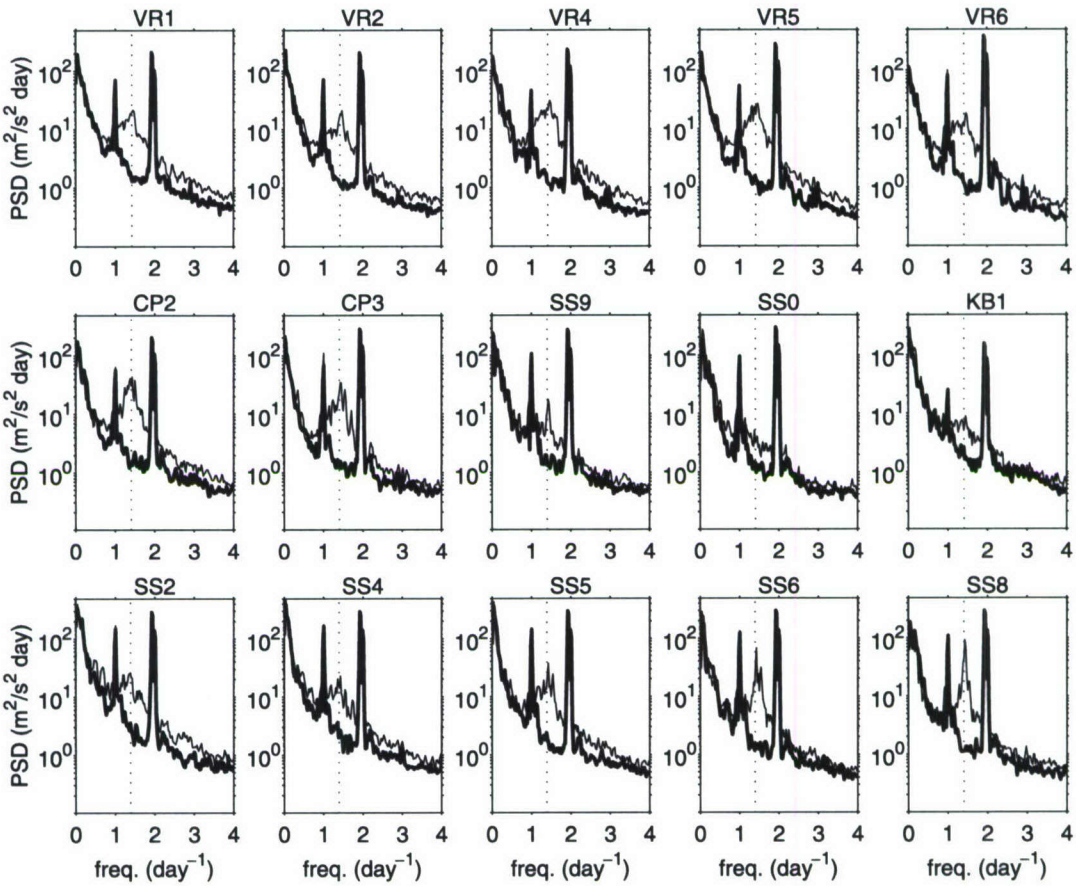

Figure 10. Vertically averaged rotary spectra of the JRP ADCP data prior to detiding and filtering. The positive (counterclockwise) rotary spectra are drawn as thick lines and the negative (clockwise) rotary spectra are drawn as thin lines. The vertical dotted lines indicate the frequency of inertial oscillations at each station.

median for all sites of the ratio $\overline{(1/N)\sum_{z=1}^{N} EKE^*(z,t)}$ to $\overline{\mathrm{EKE}^{\ddagger}(t)}$ decreases from 1.1 to 0.6 from October through December, ranges from 0.4 to 0.3 in January through March, and peaks to 1.8 for April. In April the median ratio of $\overline{(1/N)\sum_{z=1}^{N} EKE^*(z,t)}$ to MKE‡ is above 12.

[44] The square root of 2 times $\overline{\mathrm{EKE}^*(z,t)}$ is displayed in Figure 13 to show the depth structure of the vertically varying eddies. The factor of 2 and the square root is used for easier comparison to Figure 9. The velocity range for Figure 13 is double that of Figure 9 illustrating the fact that $\overline{\mathrm{EKE}^*(z,t)}$ is greater than MKE*(z) at all locations, all depths, and all months with the only exception of the bottom 2 m of site SS2 in January. Energy is surface intensified at many sites, especially at sites SS2–5, CP2–3, and VR1–4. October and April tend to have higher $\overline{\mathrm{EKE}^*(z,t)}$ than other months.

[45] However, especially for April, much of this higher energy is due to the presence of near-inertial waves. The contribution of oscillations from this frequency band was estimated by calculating the energy terms from velocities after the application of a fourth-order stop band filter run forward and backward using cutoff frequencies of 1.2 and 1.9 cycles per day (inertial oscillation frequency is 1.4 cycles per day). Figure 14 shows the percentage of $\overline{(1/N)\sum_{z=1}^{N} \mathrm{EKE}^*(z,t)}$ that can be explained by energy in this frequency band. The percentages are especially high for all stations in April and for stations SS5, SS6, and SS8 in October. Near-inertial energy is a relatively high percentage of the vertically varying eddy energy at site CP2 for all months and at the VR moorings for all months except January and February. Removing the near-inertial oscillations lowers the ratio of $\overline{(1/N)\sum_{z=1}^{N} \mathrm{EKE}^*(z,t)}$ to other energy terms but the only qualitative change is a reduction in the relative magnitude of the October and April peaks. Also, $\overline{\mathrm{EKE}^*(z,t)}$ is still greater than MKE*(z) for all but five of the 3801 (1 m) bins across seasons and stations.

[46] Figure 15 shows the relative contributions of each of the terms of equation (3) to the vertical average of the monthly averaged total kinetic energy per unit mass. Near-inertial oscillations have been filtered out of these results as described in the previous paragraph. With the exception of sites SS2, VR1, and VR2 in March and April, spatial variance is generally greater than seasonal variance. In the WAC, over 50% of kinetic energy generally comes from vertically uniform mean flows, around 30% from vertically uniform eddies, and over 10% from vertically varying eddies. In contrast, the contributions in the EAC are around

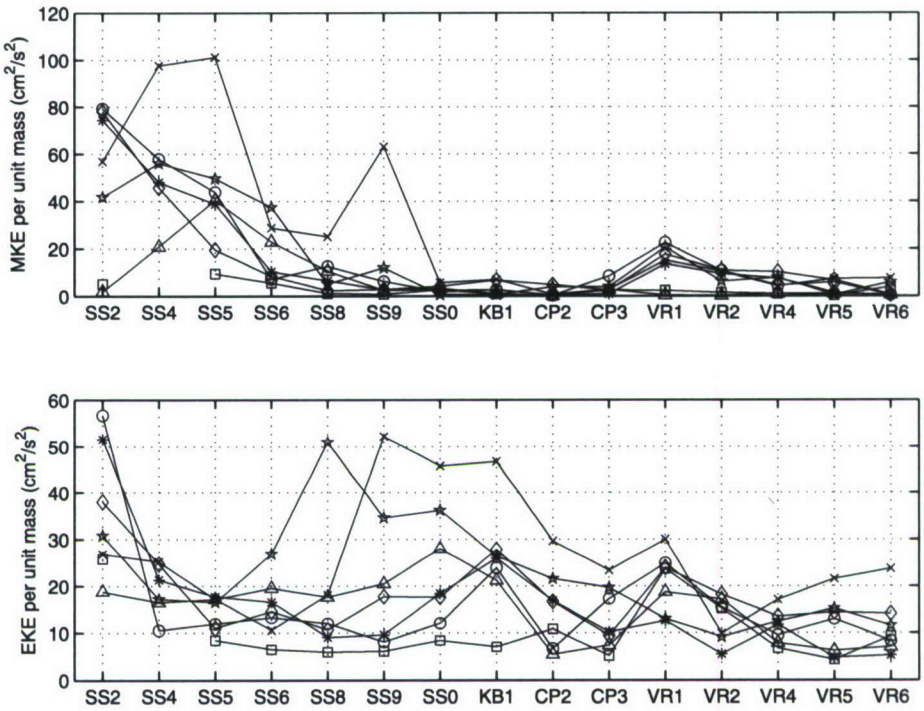

Figure 11. Monthly means excluding strong storm periods of MKE‡ (top) and $\frac{1}{T}\sum_{t=1}^{T}$ EKE$^{\ddagger}(t)$ (bottom). Lines for different months are delineated by the following: crosses for October, stars for November, diamonds for December, asterisks for January, circles for February, triangles for March, and squares for April.

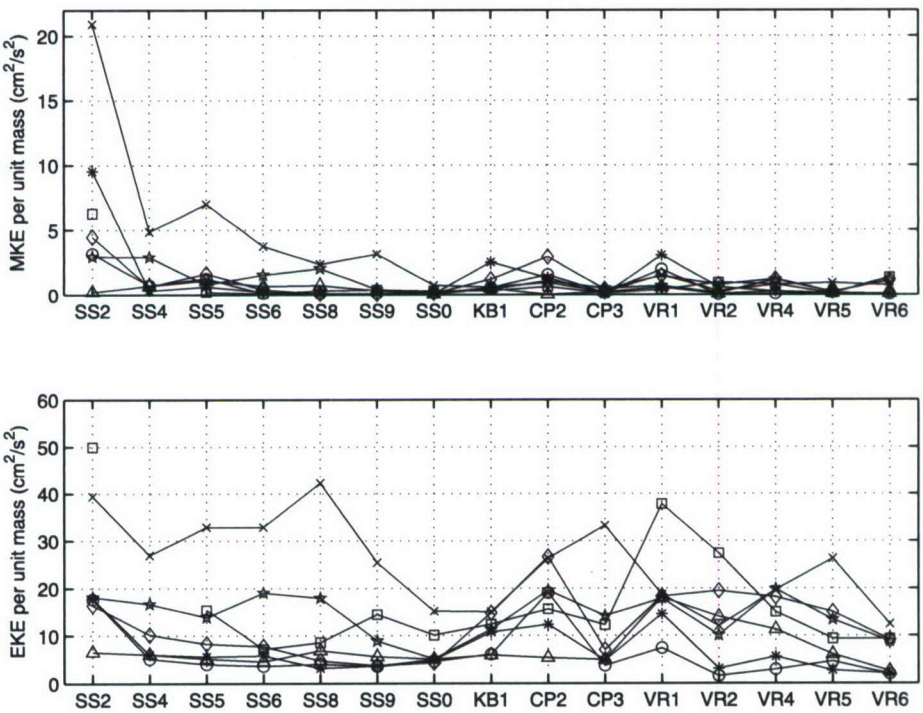

Figure 12. Monthly means excluding strong storm periods of $\frac{1}{N}\sum_{z=1}^{N}$ MKE*(z) (top) and $\frac{1}{TN}\sum_{t=1}^{T}\sum_{z=1}^{N}$ EKE*(z, t) (bottom). Lines for different months are delineated by the following: crosses for October, stars for November, diamonds for December, asterisks for January, circles for February, triangles for March, and squares for April.

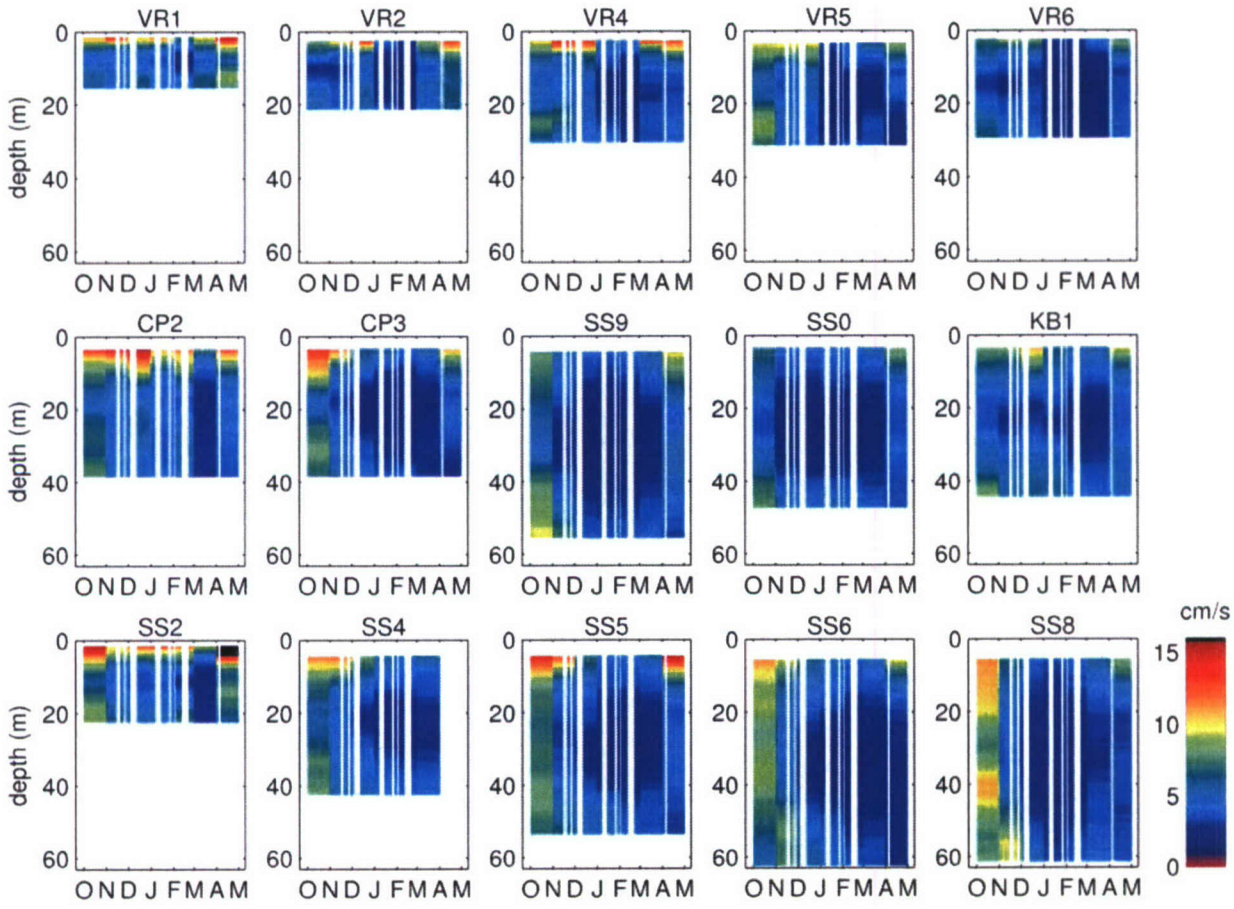

Figure 13. As in Figure 9, but colors are the square root of 2 times $\frac{1}{T}\Sigma_{t=1}^{T}$ EKE*(z, t) (monthly mean).

20% from vertically uniform mean flows, around 60% for vertically uniform eddies, and over 15% for vertically varying eddies. For the moorings in the middle of the northern Adriatic (CP2 3 and KB1), even higher percentages of the total kinetic energy were from eddy terms with generally less than 10% from vertically averaged mean flows, around 60% from vertically uniform eddies, and around 30% from vertically varying eddies. Along the VR mooring line from Venice to Istria, the contribution from vertically uniform mean flows generally decreased from 40% to 10%, the contribution from vertically uniform eddies increased from 40% to 60%, and the contribution from vertically varying eddies was typically 20% or higher.

6. Strong Storms

[47] In the northern Adriatic, strong storms drastically alter the circulation. Their effect is pronounced enough to influence both seasonal and annual means. During the study period, −0.0425 Sv (29%) of the −0.1470 Sv mean outflow transport along the Italian slope is due to the occurrence of strong storms. The average transport (including spin-up and spin-down times) was −0.2806 Sv for strong bora periods and −0.3092 Sv for strong sirocco periods. The bora average is probably a more accurate representation of average conditions than the sirocco average as it represents an average over 38 days divided among 10 transport peaks

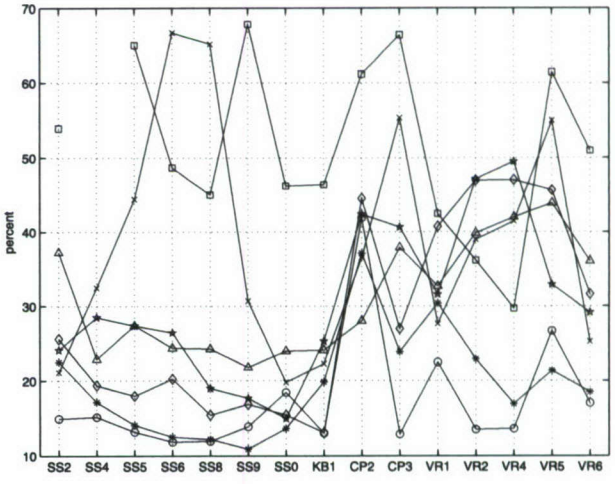

Figure 14. Percentages by month of the portion of $\frac{1}{TN}\Sigma_{t=1}^{T}\Sigma_{z=1}^{N}$ EKE*(z, t) that is produced by energy in the frequency band between 1.2 and 1.9 cycles per day. Lines for different months are delineated by the following: crosses for October, stars for November, diamonds for December, asterisks for January, circles for February, triangles for March, and squares for April.

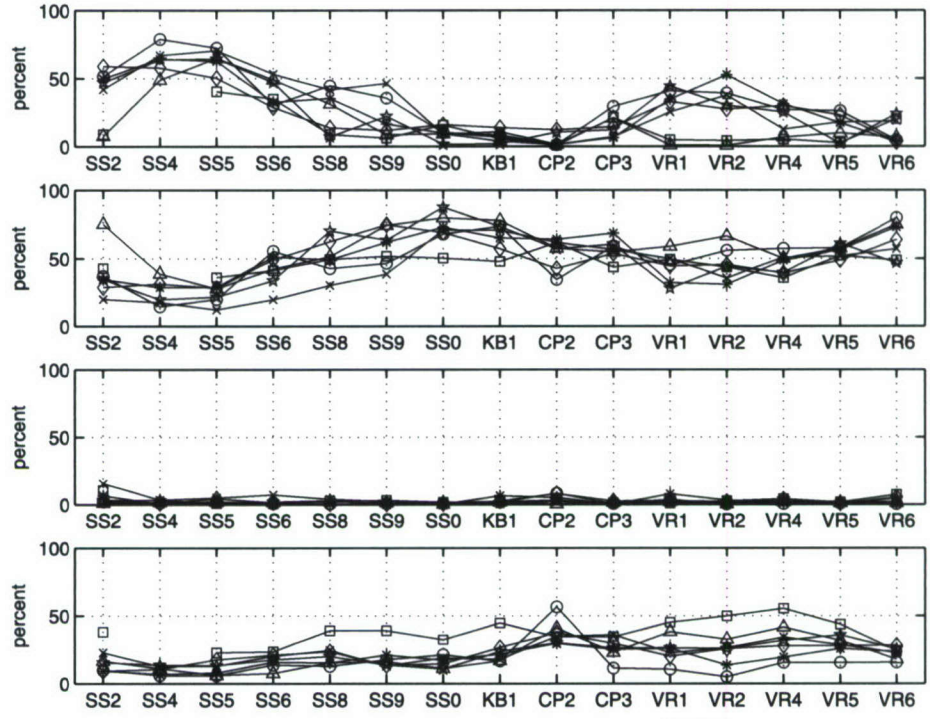

Figure 15. Excluding near-inertial oscillations, percentages of $\overline{\mathrm{TKE}^{\ddagger}}$ contributed by $\mathrm{MKE}^{\ddagger}$, $\frac{1}{T}\sum_{t=1}^{T}\mathrm{EKE}^{\ddagger}(t)$, $\frac{1}{N}\sum_{z=1}^{N}\mathrm{MKE}^{*}(z)$, and $\frac{1}{TN}\sum_{t=1}^{T}\sum_{z=1}^{N}\mathrm{EKE}^{*}(z,t)$ from top to bottom, respectively. Lines for different months are delineated by the following: crosses for October, stars for November, diamonds for December, asterisks for January, circles for February, triangles for March, and squares for April.

compared to an average over 9 days divided among three transport peaks. As the numbers of strong storms vary considerably from year to year, the mean outflow of the WAC should also exhibit considerable interannual variability. However, an estimate for adjusted WAC outflow could be made for a different year by adjusting the base outflow of −0.1045 Sv by weighted averages of the bora and sirocco means on the basis of days of occurrence.

6.1. Average Sirocco and Bora Currents

[48] Using the strong storm index of section 3.3, the mean circulation for strong sirocco and strong bora storm periods of 22 September 2002 through 5 May 2003 can be calculated. Figure 16 and Tables 3 and 4 show the results. Note that the velocity scale for Figure 16 is one half that of Figures 4–7, for clarity in displaying these much stronger circulations.

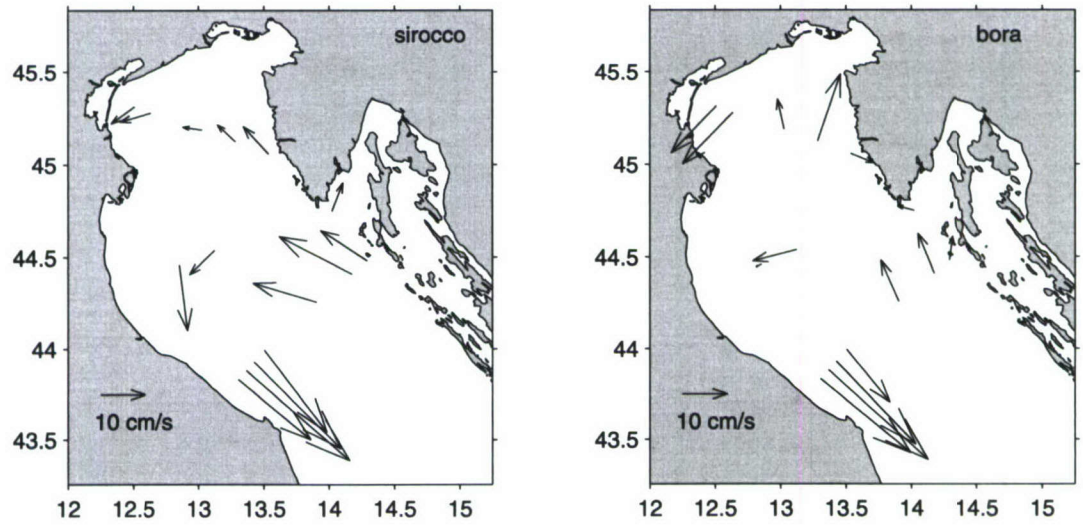

Figure 16. Mean vertically averaged currents over strong sirocco storm periods (left) and over strong bora storm periods (right).

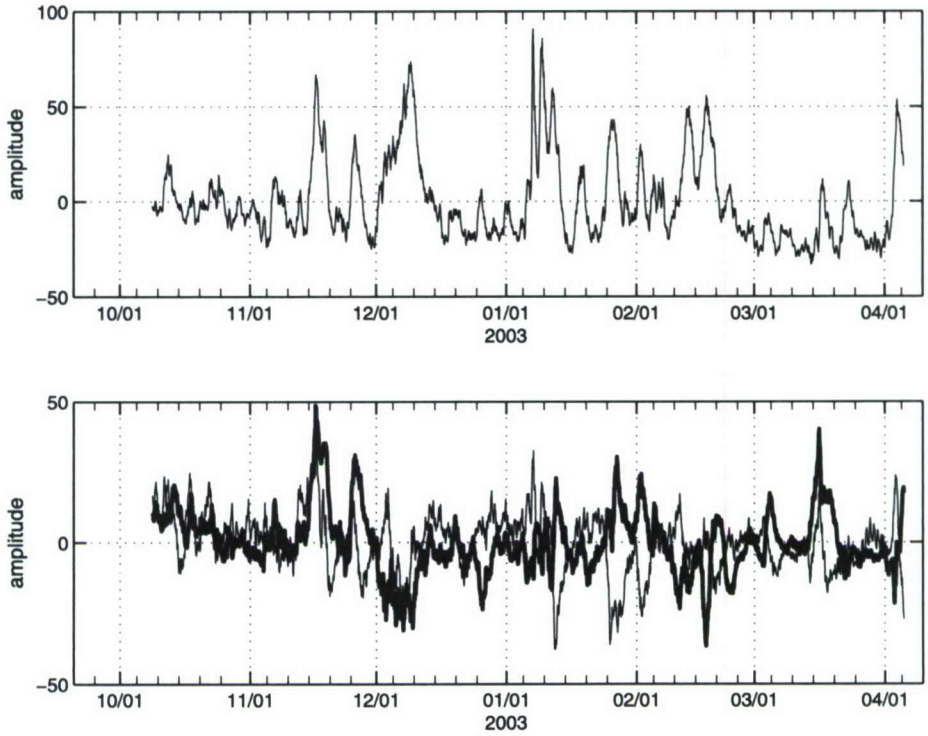

Figure 17. EOF mode 1 (top), mode 2 (bottom; thick line), and mode 3 (bottom; thin line) time amplitudes. Minor tick marks denote the 5th, 10th, 15th, 20th, and 25th of each month.

[49] The average sirocco circulation (Figure 16, left) has a very strong EAC/WAC system with peak flow at site SS4 in the WAC and at site SS9 in the EAC. Cyclonic turning/closure of the gyre occurs around sites CP2 and CP3. Vertically averaged flows in the WAC are accelerated directly against the direction of sirocco winds. Turning of flow in a cyclonic type pattern also occurs at sites VR4–6 although this northern system is not as strongly excited as the southern cyclonic gyre. Flow is moderate at sites KB1, VR1, and VR2, directed into Kvarner Bay at site KB1 and toward the southern Venice Lagoon inlet at sites VR1–2.

[50] The average bora circulation (Figure 16, right) is similar to the sirocco circulation in that the EAC/WAC system is accelerated, but there are many distinct differences in the two patterns. The WAC pattern is very similar to the WAC pattern of the sirocco, but with slightly faster flows at the inshore site (SS2). The EAC is quite different as it tilts toward Kvarner Bay during bora instead of tilting toward Italy as observed during sirocco. Under bora conditions, vertically averaged flow in the north entrance to Kvarner Bay (site KB1) is weakly directed outward toward Istria in the mean. Flow at site CP3 is directed toward the Italian coast and a stagnation point occurs at site CP2. Currents at sites VR1–5 suggest a strong northern cyclonic cell. The flow from VR5 to VR6 has rotated clockwise providing evidence for the existence of an anticyclonic circulation cell against Istria in mean bora conditions.

6.2. EOF Analysis

[51] To examine the overall storm contribution to the variability of the currents beyond the WAC sites of SS2–6 considered in section 3, an empirical orthogonal function (EOF) analysis was performed for the complete set of vertically averaged velocities measured from the JRP moorings. Eigenvectors and time-dependent amplitudes (eigenfunctions) were calculated using the singular value decomposition technique described by *Emery and Thomson* [1997].

[52] The first EOF mode explains 40.4% of the variance and it has a clear physical interpretation. Figure 17 (top) shows the time amplitude of the first mode. This time series has a remarkable correspondence to peaks in WAC outflow along the Italian slope (Figure 3, top) with a 0.93 correlation coefficient between these two time series. The spatial pattern of the eigenvectors for mode one is shown in Figure 18 and is very similar to the mean bora ocean response (Figure 16, right). Excitation of flow in the bora pattern is the source of highest variability considering all JRP mooring sites. The three sirocco peak excitations also correspond to peaks in EOF mode one excitation. This reflects the similarities between bora and sirocco excitation.

[53] EOF modes two and three explain 11.0% and 9.4% of the variance, respectively (Figure 17, bottom). Their amplitudes peak together during the beginning of the sirocco periods, then mode two excitation decays to zero and mode three amplitudes peak in the negative direction as the sirocco event evolves with time. When the modes vary in this way, they represent corrections to the bora excitation pattern (mode one) that transform it into the sirocco excitation pattern. However, the spatial pattern of mode two or mode three alone does not have a clear physical interpretation.

[54] EOF modes two and three also illustrate the variability in the excited circulation patterns caused by different

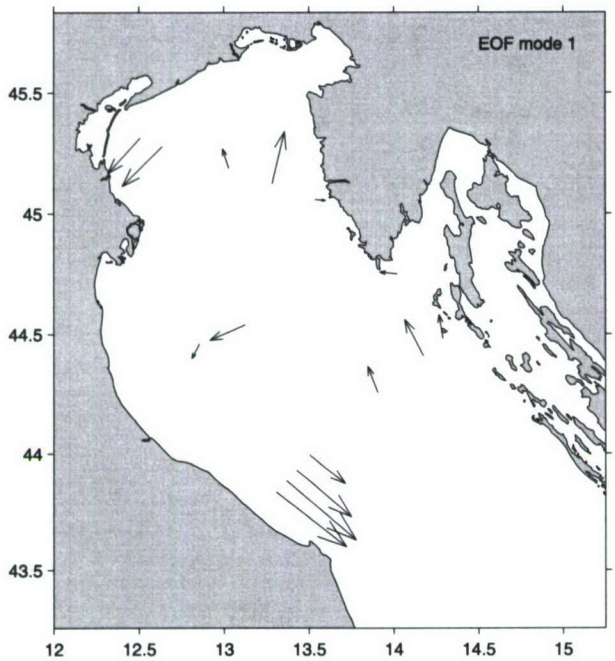

Figure 18. Spatial structure function of currents for EOF mode 1.

bora. Modes two and three sometimes have positive or negative peaks that are relatively strong during bora peaks but the pattern is not consistent for different bora periods or even for different bora peaks within a bora period. That is, for individual times the bora circulation that was measured often had second-order departures from the field shown in Figure 18.

7. Discussion

[55] From October 2002 through April 2003 the northern Adriatic experienced extended periods of strong wind forcing that caused the circulation to depart drastically from typical strengths and patterns (Figure 2). Blending such times into monthly circulation means produces fields that are representative of neither the strong wind response circulation nor the general circulation and thereby masks features of both circulations. The circulation process is not stationary or ergodic over monthly timescales; and statistical means are very sensitive to the number and timing of storms for a given year. By calculating separate statistics for the storm and nonstorm periods, this sensitivity is removed and mean fields are more likely to match observed conditions for particular times and be applicable to other years. This dynamics-based averaging applied to currents is similar to the concept of using a mode-based climatology for hydrographic data described by *Jeffries and Lee* [2007].

[56] Although the JRP mooring measurements cover only a particular year and therefore the results should be interpreted with considerations of interannual variability, it is still useful to compare these results to other climatologies of the Adriatic. Particularly, there are differences between how the seasons of the Adriatic are defined in other works. For example, *Artegiani et al.* [1997a] define the seasons as January–April (winter), May–June (spring), July–October (summer), and November–December (fall) on the basis of relative heat storage from hydrographic data, while *Poulain* [2001] defined the seasons as January–March (winter), April–June (spring), July–September (summer), and October–December (fall) on the basis of kinetic energy from drifter data. The definition of *Poulain* [2001] is more applicable to circulation means as the seasons are determined by a circulation parameter rather than a thermohaline parameter. However, as strong wind storms have a major impact on the kinetic energy, the definition of *Poulain* [2001] is likely to be sensitive to the average frequency of strong storms for particular months. Another reason that the kinetic energy season definition may be less valid for our monthly means is that the seasons for the whole Adriatic may not be appropriate for the subbasin of the northern Adriatic. The northern Adriatic is roughly only one third of the area used to calculate drifter kinetic energy.

[57] The effect of strong storm frequency on the drifter seasons was estimated using a simple calculation with QUIKSCAT winds from 1999–2006. Winds from 44.375°N, 13.625°E that exceeded 10 m/s were used to identify storms. Storms were classified as bora if winds were from the northeast quadrant and as sirocco if winds were from the southeast quadrant. The average frequency for each month and each September May period was compiled from these results. The average frequencies of sirocco and bora peak in November and December, respectively, under these definitions. *Poulain* [2001] found that the average total kinetic energy peaked in December, the month of the QUIKSCAT bora peak. However the drifter kinetic energy decreases more rapidly in January from the peak value than the QUIKSCAT decrease in bora frequency.

[58] For 2002/2003, our monthly mean results excluding strong storm periods (Figures 4–7 and 9) show a seasonal separation of October, December through February, and March through April. October generally has more kinetic energy (Figure 11) and vertical structure (Figure 9) than other months. The EAC/WAC system is relatively very strong, the northern cyclone is relatively strong, and flow is out of Kvarner Bay at KB1. The means of December through February are qualitatively similar. The EAC/WAC system is relatively strong, the northern cyclone is relatively strong, flow is out of Kvarner Bay at KB1, and mean currents have relatively little vertical structure away from the coastal sites near Italy and site KB1. However the circulation at sites CP2 and CP3 do show month to month differences in this period. The vertically averaged means for March and April have similar relatively weak EAC/WAC systems, no discernable northern cyclones, and inflow at site KB1. However, April had a larger percentage of kinetic energy in the near-inertial band than March.

[59] The monthly mean maps excluding strong storm periods should not be interpreted as nonbora/nonsirocco northern Adriatic circulations. COAMPS wind fields and Figure 3 clearly show the presence of bora wind events that have not been excluded. Weak and transient bora and sirocco events occur to some degree during every period and increase the general variability of the circulation. It is not practical or desirable to remove these contributions from the means and variances because the ocean response does

not reach a fully developed separate state during the events as it does for the strong storms.

[60] The mean circulation for November differs qualitatively from both the October pattern and the December–February pattern. This could be caused by a true seasonal difference as the northern Adriatic stratification erodes or it could be caused by the extreme Po River outflow event during the latter half of November 2002. The Po was measured at a peak flow rate of 7960 m^3/s on 30 November compared to the winter average of 1500 m^3/s reported by *Raicich* [1994]. The flow pattern toward Croatia at site CP2_3 is different than the patterns at these sites for other months. This difference and the closeness of these stations to the normal Po plume path suggest that the flood may be determining the flow there. In November the WAC and Italian side of the northern cyclone remain well defined, but the average flow is somewhat more variable on the Croatian side of the basin. The second half of the Po flood event occurs in December. However, the December means average over relatively little of the Po flood period as much of it is excluded by the occurrence of the strong bora storm during 3–12 December (Table 2).

[61] It is unclear if the influence of the river flooding could explain the winter peak in mean and eddy vertical current structures observed at stations VR1, CP2, SS2, and KB1 (Figures 9 and 13). VR1, CP2, and SS2 are the stations closest to the Italian coast where the Po plume should be found most often, but the fresh waters from the flood in November/December would have to have a long residence time in order to affect the February means. Perhaps the circulations of the frequent bora during this period act to trap fresh water in the northern Adriatic. KB1 is near the Raša River. *Orlić et al.* [2006] document a peak in this river's outflow in November 2002. Similarly to the other sites, this river peak could explain the winter peak in current vertical structure if the residence time of fresh water in Kvarner Bay is relatively long. However since this site is close to the general location of the Istrian front where the warmer waters of the EAC turn northwestward, stratification is more likely caused by frontal dynamics and slumping as observed by *Lee et al.* [2005a] in February.

[62] The kinetic energy calculations suggest a seasonal cycle in the WAC with high energies in October, moderate energies from November through February, and weaker energies in March and April. WAC kinetic energy is approximately evenly divided between mean and eddy forms with the greatest percentage of noninertial eddy energy associated with vertically uniform variations. These variations are likely caused by WAC meanders. A seasonal cycle is also suggested for the EAC energies, with higher energies in October and November than other months. However kinetic energy is mainly in the form of vertically uniform eddies (meanders). This supports the conventional view of a weaker more diffuse and varying current.

[63] A seasonal cycle is less clear for the region southeast of the Po River and for Kvarner Bay, but there is a general kinetic energy decrease from October through April. Mean kinetic energy is universally low for these regions, but eddy kinetic energy causes the total kinetic energy to reach values similar to those at other non-WAC sites.

[64] In the northern cyclonic gyre region a clear seasonal cycle is not evident with respect to kinetic energy, although the total kinetic energies closer to Istria are generally higher from October through December than from January through April. Mean kinetic energy is generally lower than eddy kinetic energy in the region, especially close to Istria. Significant amounts of eddy kinetic energy are from vertically varying currents and somewhat less than half of these latter energies are due to near-inertial waves (except in January and February). The disappearance of the northern cyclone near Venice in March and April is accompanied by an increase in vertically varying eddies from both near-inertial waves and other sources.

[65] *Ursella et al.* [2006] produced mean and eddy kinetic energy maps for the northern Adriatic from surface drifters deployed in 2002 and 2003. They analyzed the energies by season and separately by various wind storm periods and low-wind Po River flood and nonflood times. Comparisons between their results and Figures 11–15 are problematic because of differing methodologies as their maps for fall and winter include strong storms and their maps for low-wind conditions are separated by high and low Po outflow conditions. Regardless, our results do demonstrate (Figures 12 and 13) that eddy kinetic energy at the surface may be considerably higher than the vertical average of eddy kinetic energy.

[66] The observed vertical structure of kinetic energies for October suggest that the water column was more stratified than in other months at most sites. In contrast, the lack of vertical structure in the mean currents and kinetic energies for the period of December (excluding the Po flood/bora period) through March suggests that the water column was typically unstratified at most sites. Even though only slight (monthly) mean vertical shear was observed, the increased relative occurrence of near-inertial waves at all sites in April suggests that waters have begun to restratify. The CTDs taken near JRP mooring sites support these conclusions. For the period September 2002 to May 2003, higher levels of stratification were observed for the months of September, October, April, and May. Limited number of CTD profiles showed generally very weak stratification from November through March.

[67] Some new observational details emerge from the mean circulation field calculated only from times of strong ocean response to bora storm events. Strengthening of the WAC during bora was observed by programs in the 1980s [see *Cushman-Roisin et al.*, 2001] and further documented by *Book et al.* [2005]. The mean bora circulation (Figure 16) shows not only enhanced flow in the EAC/WAC gyre but a distinct tilt in the EAC toward Kvarner Bay. NCOM predictions of cross-basin flow near Ancona and the production of meanders in the EAC in the region south of Kvarner Bay [*Martin et al.*, 2006] qualitatively agree with this observed tilt, but other possible circulation patterns cannot be ruled out. Our results also imply considerable spatial variance of flow southeast of the Po as the mean at CP3 is directed toward Italy but a short distance away (at site CP2) the flow has nearly zero mean.

[68] *Sturm et al.* [1992] and others have observed the northern cyclone in satellite images during bora. Our mean field shows significant strengthening of this gyre during bora. The double-gyre theoretical and modeling results have predicted bifurcation of the bottom portion of the cyclonic gyre close to Istria to form an anticyclone offshore of the

southern portion of the peninsula. Drifters have previously traced out this circulation for particular 10-day periods [*Mauri and Poulain*, 2001], but our results from VR5 and VR6 confirm the bifurcation in this region as the mean bora circulation condition. Our method of averaging over seven strong bora periods effectively illuminates this result as the observed degree of bifurcation shows considerable variance from bora to bora. A discussion of variability of bora circulation patterns is beyond the scope of this paper. *Kuzmić et al.* [2006] examine bora induced flows in more detail from two of the bora periods during winter 2003 using observational and model results.

[69] An even more intriguing result comes from the mean sirocco circulation. The EAC/WAC system is greatly enhanced for three different sirocco peaks over two different sirocco periods in November 2002. *Orlić et al.* [1994] considered the possibility of sirocco WAC enhancement using an idealized sheared wind that goes to zero at the Italian coast. However, using a more realistic wind they found a more complicated pattern of downwind flow over the Italian shelf and upwind flow over the Italian slope. The current observations taken by *Artegiani et al.* [1983] in 1981 very near the location of mooring SS2 showed weakening of the WAC circulation during the times of sirocco wind pulses implying that their mooring was located in the downwind flow regime of *Orlić et al.* [1994]. In contrast, during the November 2002 siroccos, vertically averaged flow at SS2 was strengthened in the direction of the WAC matching the strengthening observed further offshore. Averaging masks considerable depth and time variability of SS2 currents during the events and further exploration and comparison to past research is warranted. By only identifying storms that increase WAC slope transport above a threshold value, this analysis could have missed sirocco wind events that decreased WAC slope outflow. However, in Figure 3 decreases in transport not associated with flow peaks are generally not drastic, reversals are hardly present, and it would be difficult to distinguish these statistically from "normal" conditions.

[70] Other observations of the WAC at the ocean surface have found that it is weakened by sirocco. CODAR currents presented in Figures 3–10 of *Cushman-Roisin et al.* [2001] and compiled sirocco float means from *Ursella et al.* [2006] show weak currents over broader scales than could be inferred from the measurements of *Artegiani et al.* [1983]. Perhaps there is a near-surface effect; *Orlić et al.* [1994] predicts that downwind flow extends farther offshore at the surface than at depth. Regardless, our measurements show that the bulk flow of the EAC/WAC system was strengthened over a wide area and for an extended time during the siroccos of November 2002. The sirocco period from 14–20 November had the highest-WAC slope transport that was observed despite the fact that it had a much lower maximum velocity than what occurred during the bora period from January 6 to January 14 (Table 2). A dedicated reexamination of the effect of sirocco on the WAC using recent observations and new modeling tools is needed to reconcile these various results.

[71] The EOF analysis of the JRP mooring vertically averaged currents shows that the largest basin-wide, coherent source of circulation variability during the period October 2002 through April 2003 was bora-driven flow. The peaking of the (bora pattern) mode one amplitude during the strong sirocco further highlights the first-order similarities in the northern Adriatic response to bora and to sirocco. The outflow transport of the WAC over the Italian slope is an effective proxy for the amplitude variations of this mode one pattern at mooring positions dispersed throughout the northern Adriatic.

8. Conclusions

[72] ADCP current meters deployed throughout the northern Adriatic from October 2002 through April 2003 observed high levels of variability associated with wind storm events. The variability manifests itself as strong WAC transport increases along the Italian slope, with volume outflow from the northern Adriatic more than doubling its mean of 0.1470 Sv for several day periods. The WAC slope outflow time series is nearly equivalent to the calculated mode one EOF time-amplitude for the vertically averaged currents at all sites which represents the time evolution of the spatial structure that explains the largest amount of variability.

[73] If the storm variability is not removed before calculating monthly means, the means are heavily influenced by the number, strength, and duration of storms that occur in a given month and reflect neither average storm conditions nor typical nonstorm conditions. For the purpose of strong storm identification in this context it is important that they be identified from ocean parameters instead of meteorological parameters to account for ocean spin-up and spin-down times. Using this procedure, these current meter data provide the first, full depth, basin wide, monthly circulation averages for nonstorm conditions. The means of vertically averaged currents show that for October 2002 through April 2003 the EAC/WAC system was present for every month and the northern cyclone was present for all months except March and April. Circulations in October were more energetic than those in other months, circulations from December through February were of moderate energy with similar monthly average patterns, and circulations in March and April were weaker with different monthly average patterns. November circulations were transitional between October flows and winter flows with a unique cross-basin flow south of the Po toward Istria, likely caused by a Po flood. The vertical structure of currents suggests that stratification was present in October for most sites and that stratification was enhanced at the Italian coastal sites and in Kvarner Bay during winter even as other sites became unstratified.

[74] Kinetic energies in the WAC are approximately equally divided between mean and eddy terms over monthly timescales while those of the EAC are predominately from eddy terms. For the EAC/WAC system, eddy kinetic energy is mainly from vertically uniform eddies, likely caused by meanders in the system. Elsewhere in the regions of the northern Adriatic that were sampled, eddy kinetic energy was generally larger than mean kinetic energy. Vertically varying currents were important to the total kinetic energy budget through their eddy kinetic energies, but their monthly mean kinetic energies were negligible. Near-inertial oscillations contributed strongly to eddy kinetic energy in April at all sites, in all months except January and February at sites directly south of the Po and sites extending from

Venice to Istria, and in October at offshore sites in the WAC and EAC.

[75] The long-term deployment of these current meters and the identification of seven bora and two sirocco strong storm periods allowed the measurement of the first full depth, basin wide, circulation averages over these storm types. Both sirocco and bora wind storms acted to greatly strengthen the EAC/WAC system. Average bora circulations include an EAC tilt toward Kvarner Bay, a null point in the circulation south of the Po, and a double-gyre bifurcation of flow at Istria to form a cyclone/anticyclone pair. The transport of the WAC over the Italian slope reached its maximum outflow value of −0.5221 Sv during a sirocco storm while the highest nontidal velocity of 80 cm/s occurred during a bora storm.

[76] **Acknowledgments.** We would like to thank Mark Hulbert and Ray Burge of NRL, the technical mooring team of NURC, and all those aboard RV Alliance during the adria02 and adria03 cruises for their work in the successful deployment and recovery of all the JRP moorings. Thanks to Paul Martin of NRL for providing NCOM output and displays of COAMPS winds that proved very helpful in interpretation of observations. We thank Jim Doyle as the source for COAMPS winds that we used to classify storms. We are grateful to Elio Paschini of CNR-ISMAR-Ancona and Aniello Russo of the Polytechnic University of the Marche for sharing and organizing data that they had collected. We thank Alessandro Allodi of the Parma Hydrographical Office of the Magistrate for the Po for providing Po River flow values. The entire adria23 group has been very generous with sharing of ideas, and data and this paper benefited in many ways from this openness. The Teledyne/RDI technical support staff was very helpful in reviewing and revising ADCP velocity uncertainty estimates. Thanks to Mark Wimbush for his helpful reviews. The comments from two anonymous reviewers helped to improve the quality of the paper. This work was supported by the Office of Naval Research as part of the research programs "Adriatic Circulation Experiment" and "Dynamics of the Adriatic in Real-Time" under Program Element 0602435N. This is NRL contribution JA/7330-06-6144.

References

Artegiani, A., R. Azzolini, and E. Paschini (1983), Prime considerazioni su cinque mesi di dati correntmetrici registrati in una stazione a 7 miglia a nord di Ancona (augusto–dicembre 1981), in *Atti del 5° Congresso della Associazione Italiana di Oceanologia e Limnologia*, pp. 155–163, Ital. Assoc. of Oceanol. and Limnol., Pallanza.

Artegiani, A., D. Bregant, E. Paschini, N. Pinardi, F. Raicich, and A. Russo (1997a), The Adriatic Sea general circulation. part I: Air-sea interactions and water mass structure, *J. Phys. Oceanogr.*, *27*, 1492–1514.

Artegiani, A., D. Bregant, E. Paschini, N. Pinardi, F. Raicich, and A. Russo (1997b), The Adriatic Sea general circulation. part II: Baroclinic circulation structure, *J. Phys. Oceanogr.*, *27*, 1515–1532.

Beg Paklar, G., V. Isakov, D. Koračin, V. Kourafalou, and M. Orlić (2001), A case study of bora-driven flow and density changes on the Adriatic Shelf (January 1987), *Cont. Shelf Res.*, *21*, 1751–1783.

Betello, G., and A. Bergamasco (1992), A multilevel model for the study of the dynamics of the north Adriatic Sea, in *Environmental Modeling*, edited by P. Melli and P. Zannetti, pp. 307–317, Elsevier, New York.

Book, J. W., H. T. Perkins, L. Cavaleri, J. D. Doyle, and J. D. Pullen (2005), ADCP observations of the western Adriatic slope current during winter of 2001, *Progr. Oceanogr.*, *66*, 270–286.

Book, J. W., H. Perkins, R. P. Signell, and M. Wimbush (2007), The Adriatic Circulation Experiment winter 2002/2003 mooring data report: A case study in ADCP data processing, *Memo. Rep. NRL/MR/7330-07-8999*, U.S. Naval Res. Lab., Stennis Space Center, Miss.

Cavaleri, L. (2000), The oceanographic tower Acqua Alta – activity and prediction of sea states at Venice, *Coastal Eng.*, *39*, 29–70.

Cushman-Roisin, B., M. Gačić, P.-M. Poulain, and A. Artegiani (2001), *Physical Oceanography of the Adriatic Sea: Past, Present and Future*, Springer, New York.

Dorman, C. E., et al. (2006), February 2003 marine atmospheric conditions and the bora over the northern Adriatic, *J. Geophys. Res.*, *111*, C03S03, doi:10.1029/2005JC003134, [printed 112(C3), 2007].

Emery, W. J., and R. E. Thomson (1997), *Data Analysis Methods in Physical Oceanography*, 2nd ed., Elsevier, New York.

Finizio, C., S. Palmieri, and A. Riccucci (1972), A numerical model of the Adriatic for the prediction of high tides at Venice, *Q. J. R. Meteorol. Soc.*, *98*, 86–104.

Griffin, D. A., and K. R. Thompson (1996), The adjoint method of data assimilation used operationally for shelf circulation, *J. Geophys. Res.*, *101*(C2), 3457–3477.

Guymer, T. H., and S. Zecchetto (1993), Applications of scatterometer winds in coastal areas, *Int. J. Remote Sens.*, *14*, 1787–1812.

Janeković, I., and M. Kuzmić (2005), Numerical simulation of the Adriatic Sea principal tidal constituents, *Ann. Geophys.*, *23*, 3207–3218, SRef-ID:1432-0576/ag/2005-23-3207.

Jeffries, M. A., and C. M. Lee (2007), A climatology of the northern Adriatic Sea's response to bora and river forcing, *J. Geophys. Res.*, *112*, C03S02, doi:10.1029/2006JC003664.

Kuzmić, M., and M. Orlić (1987), Wind-induced vertical shearing: ALPEX/MEDALPEX data and modelling exercise, *Ann. Geophys.*, *5B*, 103–112.

Kuzmić, M., I. Janeković, J. W. Book, P. J. Martin, and J. D. Doyle (2006), Modeling the northern Adriatic double-gyre response to intense bora wind: A revisit, *J. Geophys. Res.*, *111*, C03S13, doi:10.1029/2005JC003377, [printed 112(C3), 2007].

Lee, C. et al. (2005a), Cruise report: DOLCE VITA 1 and 2, 31 January–24 February and 26 May–15 June, 2003, *Tech. Rep. APL-UW TR 0409*, Appl. Phys. Lab., Univ. of Wash., Seattle.

Lee, C. M., et al. (2005b), Northern Adriatic response to a wintertime Bora wind event, *EOS Trans. AGU*, *86*(16), 157.

Lu, Y., and R. G. Lueck (1999), Using a broadband ADCP in a tidal channel. part I: Mean flow and shear, *J. Atmos. Oceanic Technol.*, *16*, 1556–1567.

Martin, P. J., J. W. Book, and J. D. Doyle (2006), Simulation of the northern Adriatic circulation during winter 2003, *J. Geophys. Res.*, *111*, C03S12, doi:10.1029/2006JC003511, [printed 112(C3), 2007].

Mauri, E., and P.-M. Poulain (2001), Northern Adriatic Sea surface circulation and temperature/pigment fields in September and October 1997, *J. Mar. Syst.*, *29*, 51–67.

Mooers, C. N. K. (1973), A technique for the cross-spectrum analysis of pairs of complex-values time series, with emphasis on properties of polarized components and rotational invariants, *Deep Sea Res.*, *20*, 1129–1141.

Orlić, M., M. Gačić, and P. E. La Violette (1992), The currents and circulation of the Adriatic Sea, *Oceanol. Acta*, *15*, 109–124.

Orlić, M., M. Kuzmić, and Z. Pasarić (1994), Response of the Adriatic Sea to the bora and sirocco forcing, *Cont. Shelf Res.*, *14*, 91–116.

Orlić, M., et al. (2006), Wintertime buoyancy forcing, changing seawater properties, and two different circulation systems produced in the Adriatic, *J. Geophys. Res.*, *111*, C03S07, doi:10.1029/2005JC003271, [printed 112(C3), 2007].

Perkins, H. T., F. de Strobel, and L. Gualdesi (2000), The Barney Sentinel Trawl-resistant ADCP bottom mount: Design, testing, and application, *IEEE J. Oceanic Eng.*, *25*, 430–436.

Pojc, D., and G. Hrabak-Tumpa (1982), Gale and storm winds in the Adriatic, *Acta Adriatica*, *23*, 11–20.

Poulain, P.-M. (2001), Adriatic Sea surface circulation as derived from drifter data between 1990 and 1999, *J. Mar. Syst.*, *29*, 3–32.

Pullen, J., J. D. Doyle, R. Hodur, A. Ogston, J. W. Book, H. Perkins, and R. Signell (2003), Coupled ocean-atmosphere nested modeling of the Adriatic Sea: Winter and spring 2001, *J. Geophys. Res.*, *108*(C10), 3320, doi:10.1029/2003JC001780.

Raicich, F. (1994), A note on the flow rates of the Adriatic rivers, *Tech. Rep. RF 2/94*, Inst. Sper. Trieste-Cons. Naz. delle Ric., Trieste, Italy.

Sturm, B., M. Kuzmić, and M. Orlić (1992), An evaluation and interpretation of CZCS-derived patterns on the Adriatic shelf, *Oceanol. Acta*, *15*, 13–23.

Ursella, L., P.-M. Poulain, and R. P. Signell (2006), Surface drifter derived circulation in the northern and middle Adriatic Sea: Response to wind regime and season, *J. Geophys. Res.*, *111*, C03S04, doi:10.1029/2005JC003177, [printed 112(C3), 2007].

Zore-Armanda, M., and M. Gačić (1987), Effects of bura on the circulation in the north Adriatic, *Ann. Geophys.*, *5B*, 93–102.

J. W. Book, Naval Research Laboratory, Stennis Space Center, MS 39529, USA. (book@nrlssc.navy.mil)

Richard P. Signell, U.S. Geological Survey, 384 Woods Hole Road, Woods Hole, MA 02543, USA. (rsignell@usgs.gov)

Henry Perkins, University of Maine School of Marine Sciences and Ira C. Darling Marine Center, 193 Clark's Cove Road, Walpole, ME 04573, USA. (hperkins@maine.edu)